Chemistry–A European Journal

Supporting Information

Investigating the Active Oxidants Involved in Cytochrome P450 Catalyzed Sulfoxidation Reactions

Matthew N. Podgorski, Tom Coleman, Luke R. Churchman, John B. Bruning, James J. De Voss,* and Stephen G. Bell*

Supplementary Information

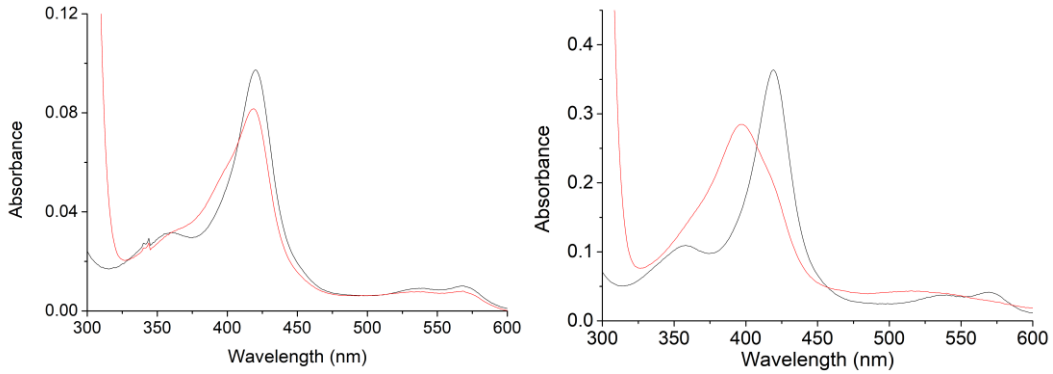

(a) D251N + 4-methylthiobenzoic acid **(b)** T252A + 4-methylthiobenzoic acid

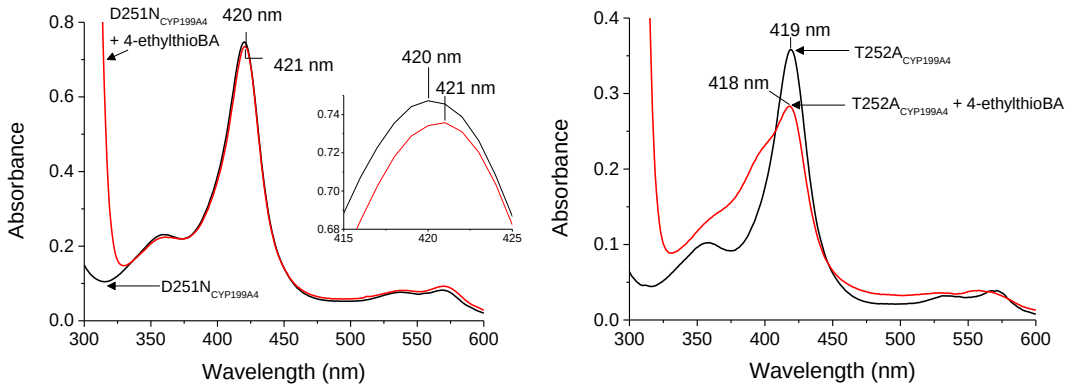

(c) D251N + 4-ethylthiobenzoic acid **(d)** T252A + 4-ethylthiobenzoic acid

Figure S1 Spin-state shifts of **(a)** $D251N_{CYP199A4}$ and **(b)** $T252A_{CYP199A4}$ induced by 4-methylthiobenzoic acid. Also shown are the shifts in **(c)** $D251N_{CYP199A4}$ and **(d)** $T252A_{CYP199A4}$ induced by 4-ethylthiobenzoic acid. The inset in **(c)** highlights the red shift of the Soret peak.

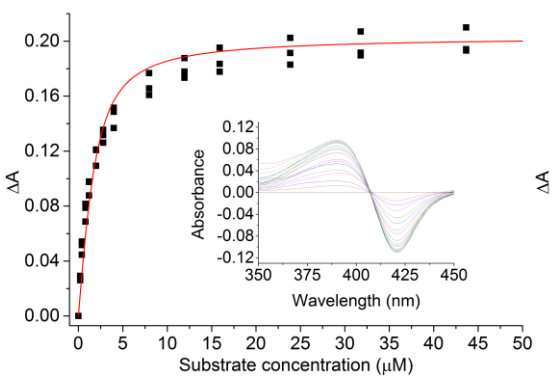

(a) D251N + 4-methylthiobenzoic acid (1.7 μM, peak: 390 nm, trough: 421 nm)

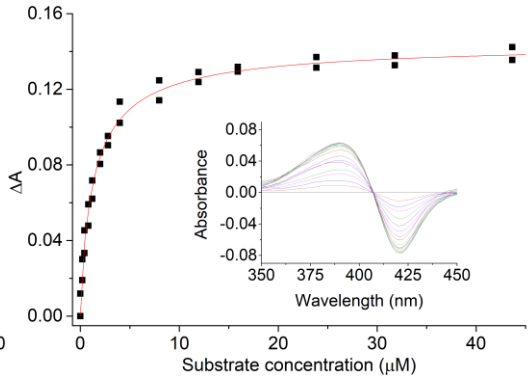

(b) T252A + 4-methylthiobenzoic acid (1.3 μM, peak: 290nm, trough: 421 nm)

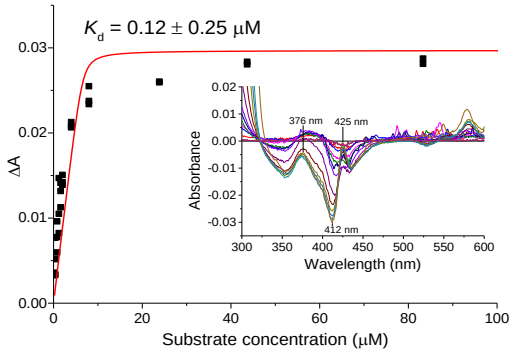

(c) D251N + 4-ethylthiobenzoic acid (6.6 μM, trough: 412 nm)

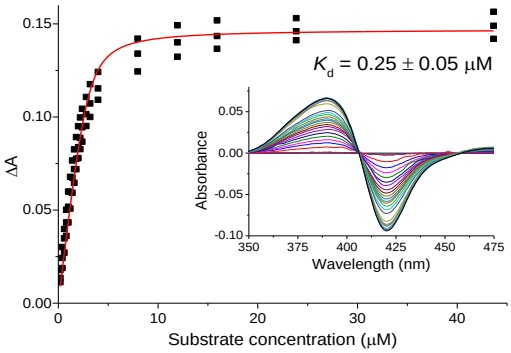

(d) T252A + 4-ethylthiobenzoic acid (3.0 μM, peak: 389 nm, trough: 420 nm)

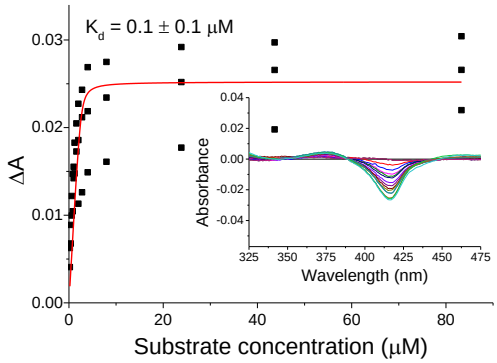

(e) T252E + 4-methylthiobenzoic acid (2.6 μM, peak: 376 nm, trough: 416 nm)

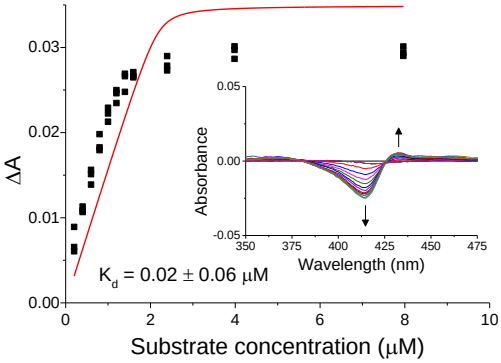

(f) T252E + 4-ethylthiobenzoic acid (2.2 μM, peak: 433 nm, trough: 414 nm)

Figure S2 UV-Vis titrations to determine the dissociation constant of **(a)** D251N$_{CYP199A4}$ and **(b)** T252A$_{CYP199A4}$ with 4-methylthiobenzoic acid. UV-Vis titrations to determine the dissociation constant of **(c)** D251N$_{CYP199A4}$ and **(d)** T252A$_{CYP199A4}$ with 4-ethylthiobenzoic acid. UV-Vis titrations to determine the dissociation constant of T252E$_{CYP199A4}$ with **(e)** 4-methylthiobenzoic acid and **(f)** 4-ethylthiobenzoic acid. The enzyme concentration used, and the peak and trough wavelengths are provided under each graph. The data were fitted to the Morrison tight-binding equation. As there is no prominent peak at 390 nm in the D251N difference spectrum in **(c)**, ΔA was taken to be A_{490}-A_{412} (baseline - trough).

Spin-state shifts of T252E$_{CYP199A4}$ induced by 4-methylthio- and 4-ethylthio-benzoic acid

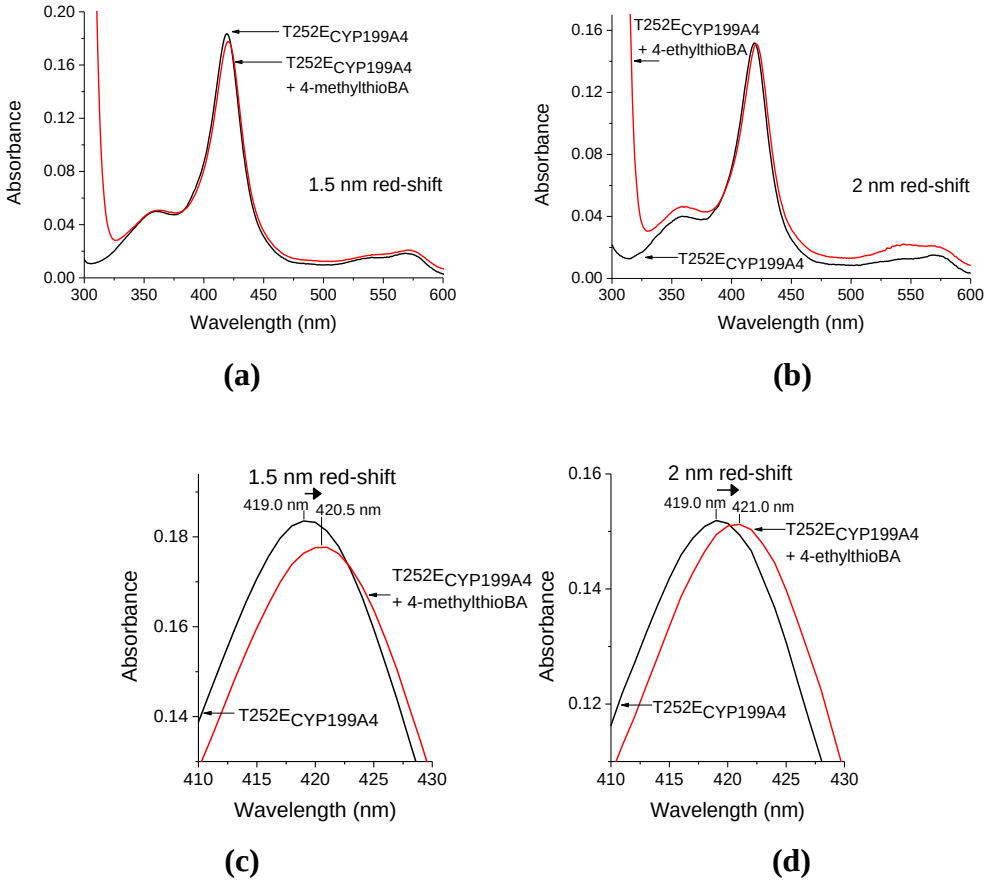

Figure S3. Spin-state shifts of the T252E mutant of CYP199A4 induced by **(a)** 4-methylthiobenzoic acid, and **(b)** 4-ethylthiobenzoic acid. These substrates induced a red-shift of the Soret band, and these red-shifts are shown more clearly in figures **(c)** and **(d)**.

Difference spectra induced by binding of sulfur ligands to $P450_{cam}$ and CYP199A4

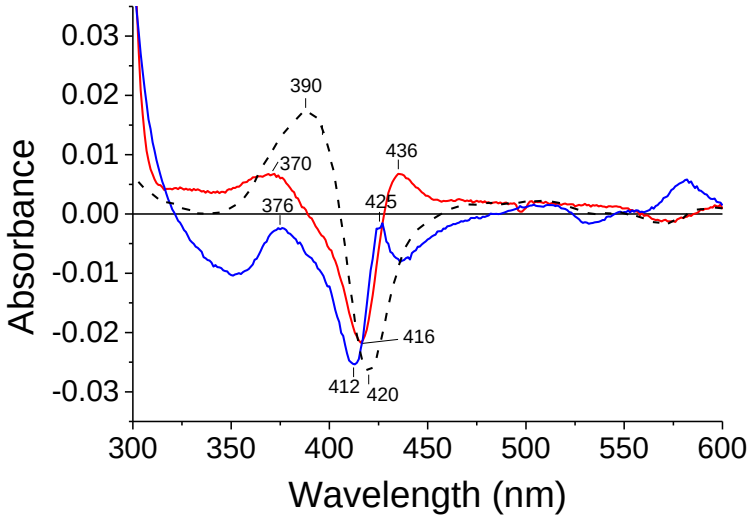

Figure S4. Difference spectra of $P450_{cam}$ with thioanisole (**red**) and $D251N_{CYP199A4}$ with 4-ethylthiobenzoic acid (**blue**). The type I difference spectrum of $T252A_{CYP199A4}$ with 4-ethylthiobenzoic acid is also shown as a **black dashed line** for comparison.

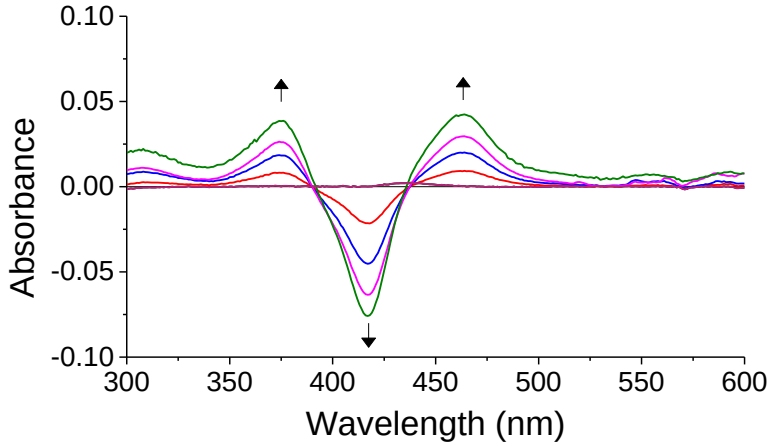

Figure S5. Difference spectra of $P450_{cam}$ with dithiothreitol (DTT).

Table S1. Features of the difference spectra of $P450_{cam}$ with thioanisole and DTT and $D251N_{CYP199A4}$ with 4-ethylthiobenzoic acid

Enzyme / Sulfide	Absorbance maxima (nm)	Absorbance minimum (nm)
$P450_{cam}$ + thioanisole	370, 436	416
$D251N_{CYP199A4}$ + 4-ethylthiobenzoic acid	376, 425	412
$P450_{cam}$ + DTT	375, 464	417

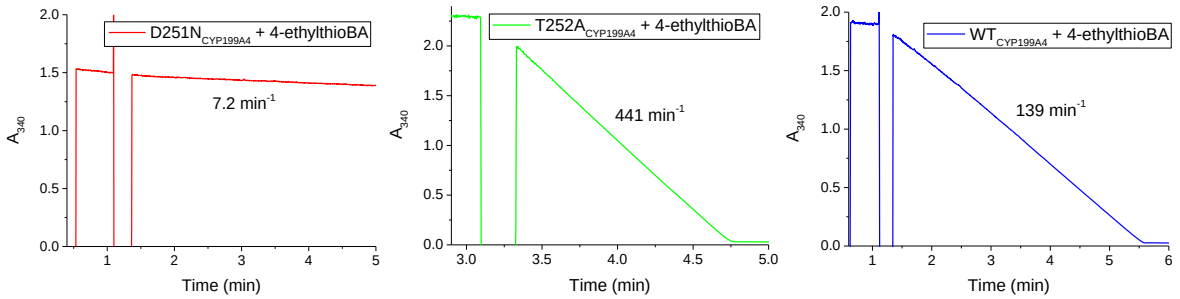

(a) D251N **(b)** T252A **(c)** WT

Figure S6. Comparison of the rates of NADH consumption by **(a)** $D251N_{CYP199A4}$, **(b)** $T252A_{CYP199A4}$ and **(c)** $WT_{CYP199A4}$ with 4-ethylthiobenzoic acid.

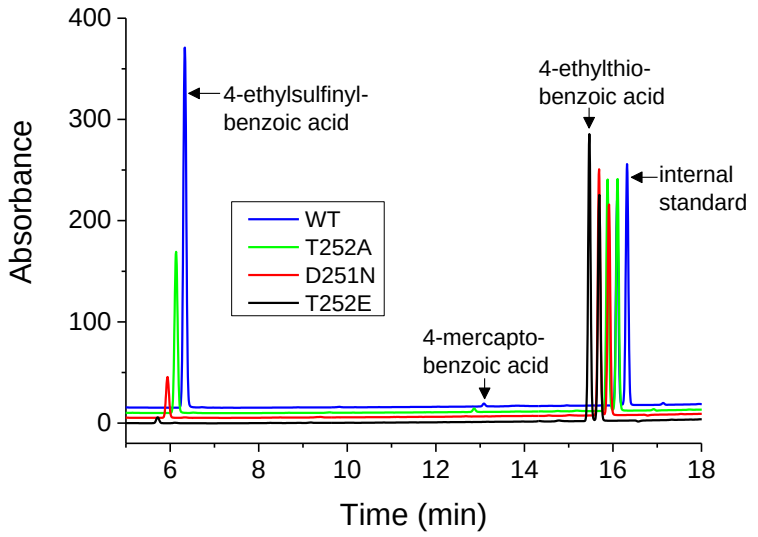

Figure S7a. HPLC analysis of the *in vitro* NADH reaction of CYP199A4 variants with 4-ethylthiobenzoic acid. The T252E, D251N, T252A and WT CYP199A4 reactions are shown in **black**, **red**, **green** and **blue**, respectively. Retention times are: 4-ethylsulfinylbenzoic acid, 5.8 min; 4-ethylthiobenzoic acid, 15.5 min; 9-hydroxyfluorene, 15.7 min. Gradient: 20 → 95% MeCN in H_2O (with 0.1% TFA). No 4-mercaptobenzoic acid was detected in the T252E or D251N turnovers. In the T252A and WT turnovers, minimal 4-mercaptobenzoic acid was formed. In the T252A turnover, the 4-mercaptobenzoic acid peak was ~2% of the size of the sulfoxide peak. In the WT turnover, it was <1% of the size of the sulfoxide peak. In the absence of an authentic sample of 4-ethylsulfinylbenzoic acid for calibration, 4-methylsulfinylbenzoic acid was used.

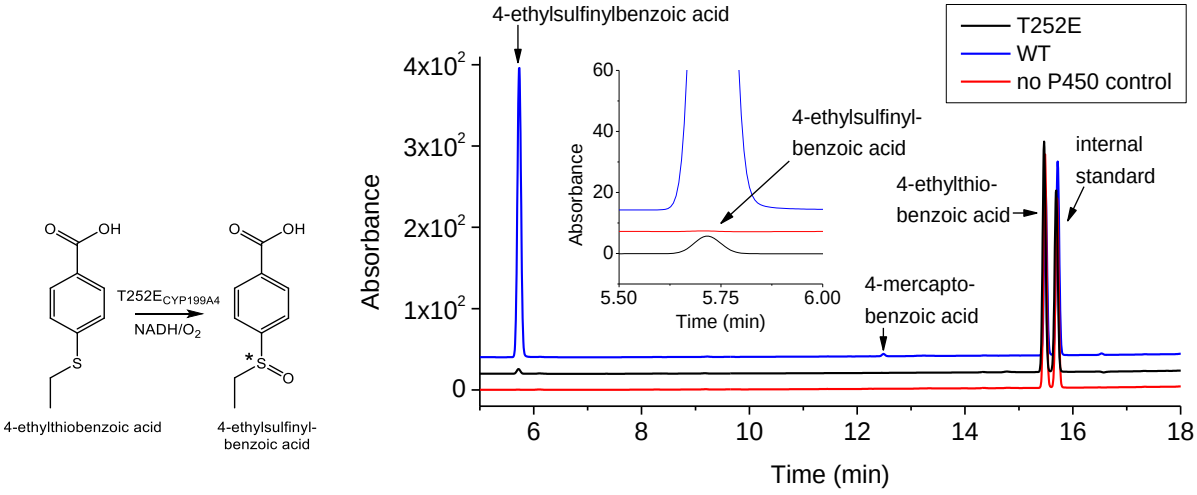

Figure 7b. HPLC analysis of the NADH/O_2-driven oxidation of 4-ethylthiobenzoic acid by T252E (**black**) and WT CYP199A4 (**blue**). In **red** is a control reaction omitting the P450. 4-Ethylsulfinylbenzoic acid appears at 5.7 min and the substrate at 15.5 min.

HPLC retention times

Table S2. HPLC retention times for *para*-substituted benzoic acid substrates and products. Gradient: 20 → 95% acetonitrile in H_2O with 0.1% TFA over 20 minutes.

Compound	Retention time (min)
4-Methoxybenzoic acid	11.4
4-Hydroxybenzoic acid	5.8
4-Methylthiobenzoic acid	13.6
4-Methylsulfinylbenzoic acid	4.7
4-Mercaptobenzoic acid	12.5
4-Methylsulfonylbenzoic acid (sulfone)	6.9
4-Ethylthiobenzoic acid	15.5
4-Ethylsulfinylbenzoic acid	5.7
9-Hydroxyfluorene (internal standard)	15.7

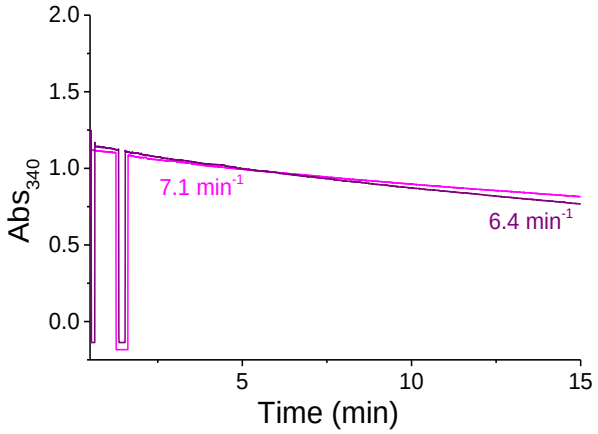

Figure S8. Rates of NADH consumption by the T252E$_{CYP199A4}$ mutant with the *para*-substituted benzoic acid substrates 4-methylthiobenzoic acid (**magenta**) and 4-ethylthiobenzoic acid (**purple**).

Co-elution of reaction products with authentic compounds to confirm their identity

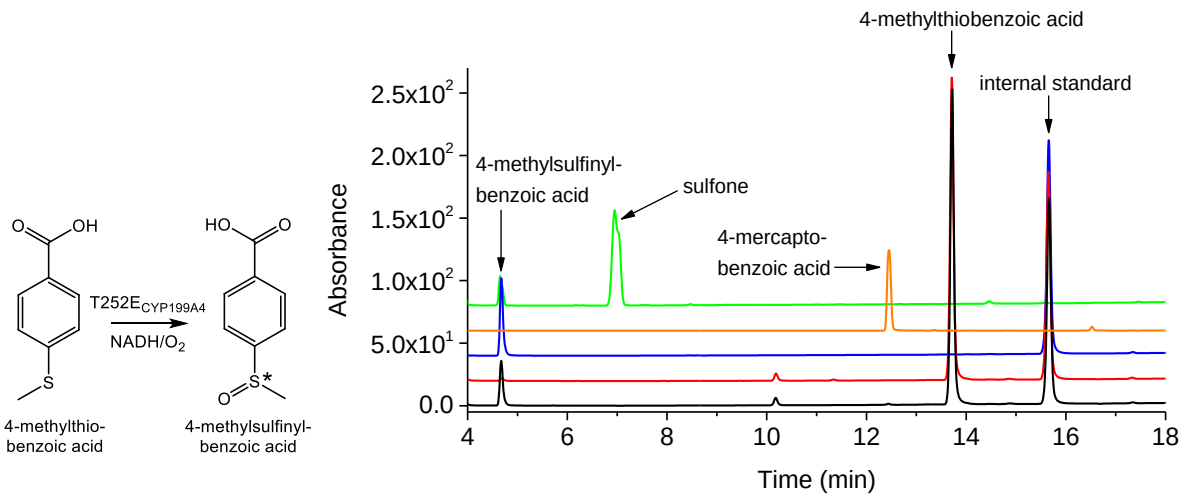

Figure S9. HPLC analysis of the NADH/O_2-driven oxidation of 4-methylthiobenzoic acid by T252E$_{CYP199A4}$ (**black**), which exclusively generated 4-methylsulfinylbenzoic acid. In **red** is a control reaction omitting the P450, and in **blue** is authentic 4-methylsulfinylbenzoic acid (RT = 4.7 min). In **orange** is authentic 4-mercaptobenzoic acid (RT = 12.5 min) and in **green** is authentic 4-methylsulfonylbenzoic acid (RT = 6.9 min); the dealkylation product and sulfone were not formed by the T252E enzyme. No 4-sulfobenzoic acid was detected. The substrate appears at 13.6 min. Gradient: 20-95% MeCN in H_2O with 0.1% TFA. Detection wavelength: 254 nm.

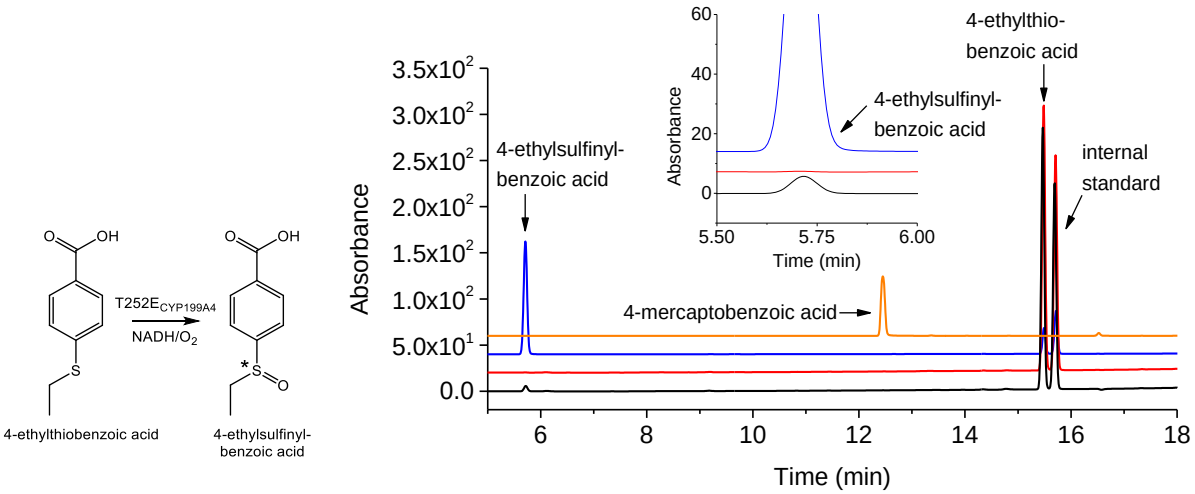

Figure S10. HPLC analysis of the NADH/O_2-driven oxidation of 4-ethylthiobenzoic acid by T252E$_{CYP199A4}$ (**black**). In **red** is a control reaction omitting the P450, and in **blue** is chemically synthesized 4-ethylsulfinylbenzoic acid (RT =5.7 min). The substrate appears at 15.5 min. Gradient: 20-95% MeCN in H_2O with 0.1% TFA. Detection wavelength: 254 nm.

H_2O_2-driven oxidation of 4-methylthiobenzoic acid by T252E$_{CYP199A4}$

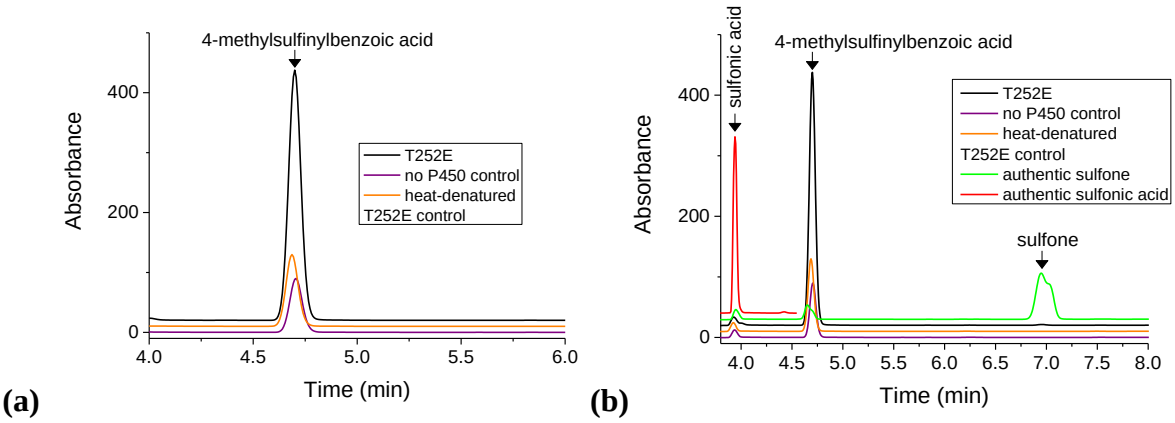

Figure 11. (a) Sulfoxidation of 4-methylthiobenzoic acid by the T252E mutant over a 20-minute period. H_2O_2 (**50 mM**) was used as the oxygen donor. The **black line** is the T252E turnover. In **orange** is the heat-denatured T252E control, and in **purple** is the no P450 control. **(b)** In **red** and **green** are authentic 4-sulfobenzoic acid and 4-methylsulfonylbenzoic acid; these products were not formed by the T252E enzyme.

Table S3a. Product generated by the T252E mutant utilizing the H_2O_2-shunt pathway during 20 min reactions. The values given are mean ± SD, with $n \geq 2$.

Substrate **BA benzoic acid**	**Product concentration (µM)**	**Average product formation rate over 20-min period** **(µM (µM-P450)$^{-1}$ min^{-1})**
4-methoxyBA	114 ± 2	1.9
4-methylthioBA	245 ± 2 [a]	4.1

Table S3b. Sulfoxide concentration in the T252E turnover, no P450 control and heat-denatured T252E control reactions. H_2O_2 (50 mM) was used as the oxygen donor and the reaction time was 20 minutes.

Substrate	**Product concentration (µM)**		
	T252E turnover	**no P450 control**	**heat-denatured T252E**
4-methylthioBA	311 ± 2	66 ± 1	86

[a] The 4-methylsulfinylbenzoic acid concentration in the reaction mixture was 311 ± 2 µM and the product concentration in the no P450 control was 66 ± 1. Note that the amount of product detected in the no P450 control reactions has been subtracted from the amount of product in the T522E turnovers.

Control reactions to assess whether a Fenton-type reaction is responsible for the formation of product in the H_2O_2-driven reactions

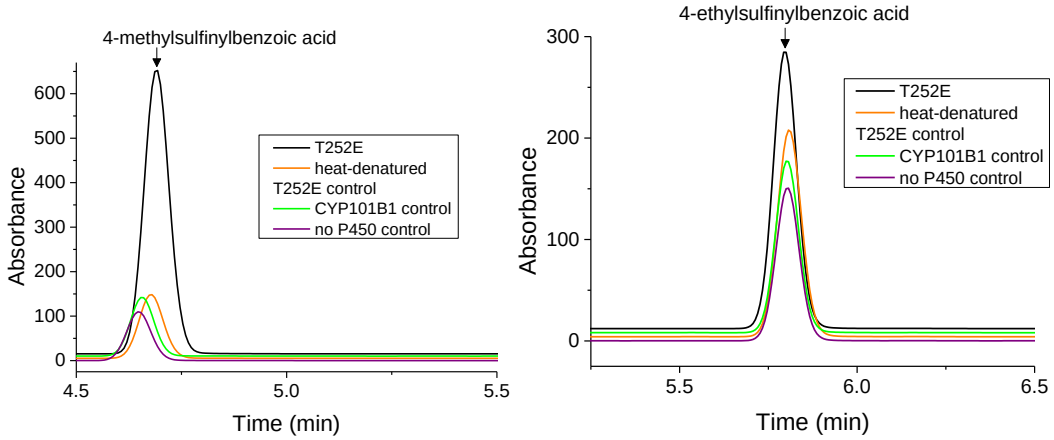

(a) 4-methylthiobenzoic acid **(b)** 4-ethylthiobenzoic acid

Figure S12. Comparison of the amount of product generated in the H_2O_2-driven T252E reactions (**black**) to the amount of product detected in the CYP101B1 control (**green**) and heat-denatured T252E control (**orange**) reactions. **The reaction time was 240 min.** The H_2O_2 concentration was 6 mM for the sulfide substrates.

Table S4. Amount of product detected in the no P450 control, CYP101B1 control and heat-denatured T252E control reactions **after 240-min reactions**. *For the thioether reactions, 6 mM H_2O_2 was used instead of 50 mM H_2O_2.

Substrate	**Product concentration (μM)**		
	no P450 control	**CYP101B1 control**	**heat-denatured T252E**
4-methoxyBA	1	1	1
4-methylthioBA *	91	92	107
4-ethylthioBA *	115	130	161

HPLC analysis of product formation by CYP199A4 isoforms driven by H_2O_2

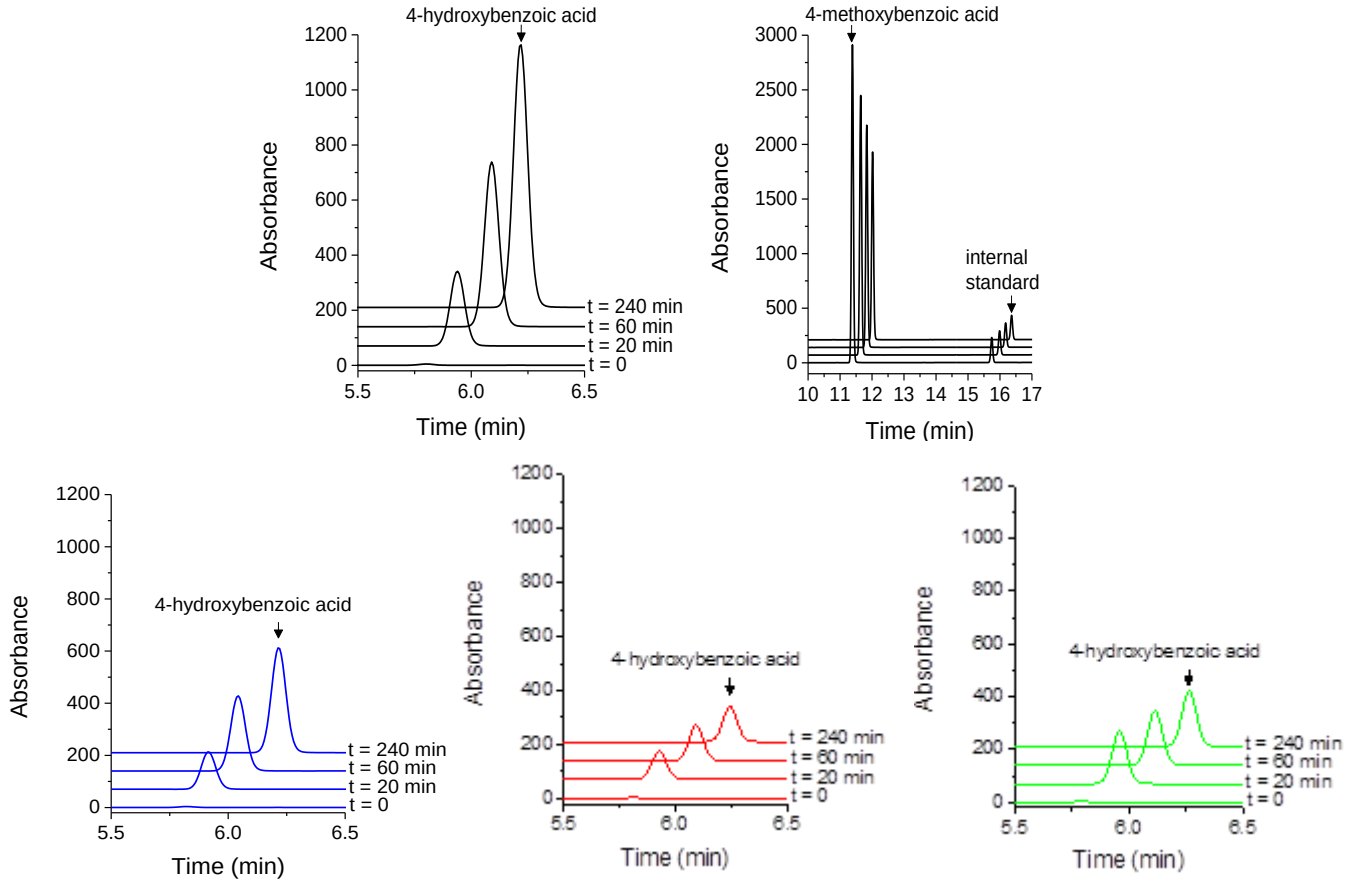

Figure S13. Conversion of 4-methoxybenzoic acid into 4-hydroxybenzoic acid by WT CP199A4 (**blue**) and the T252E (**black**), D251N (**red**) and T252A (**green**) mutants over a 4-hour period. H_2O_2 (50 mM) was used as the oxygen donor.

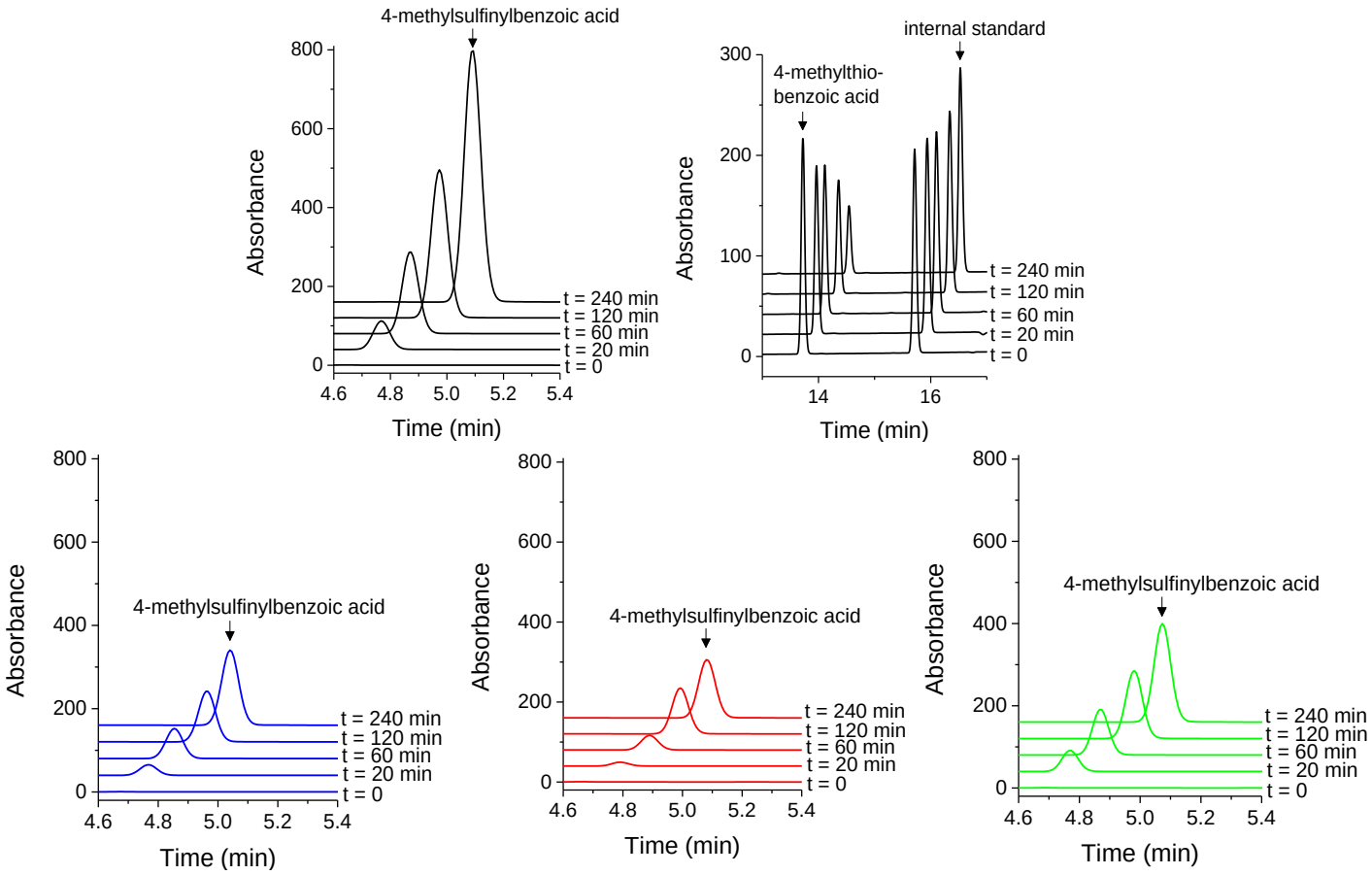

Figure S14. Conversion of 4-methylthiobenzoic acid into 4-methylsulfinylbenzoic acid by WT CP199A4 (**blue**) and the T252E (**black**), D251N (**red**) and T252A (**green**) mutants over a 4-hour period. H_2O_2 (6 mM) was used as the oxygen donor.

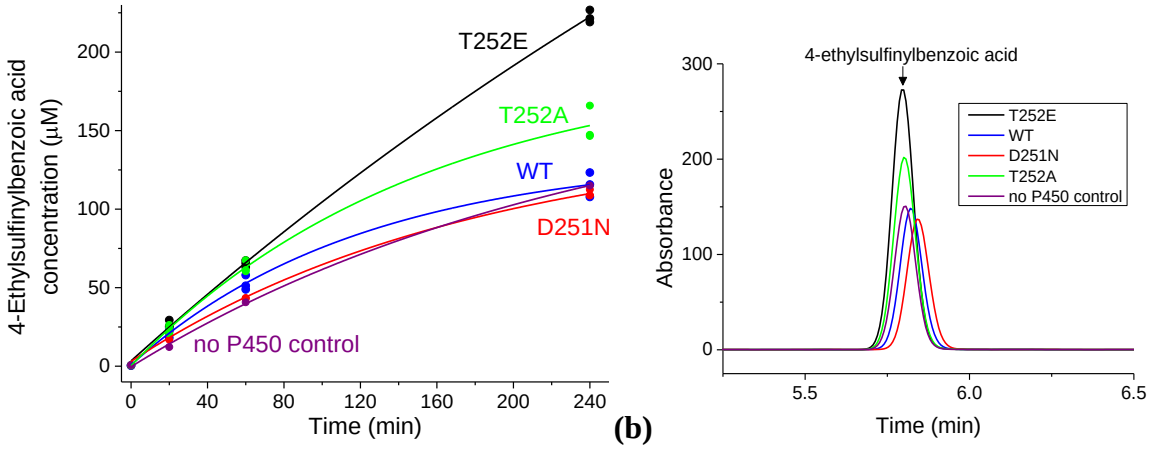

Figure S15. (a) Time course of 4-ethylthiobenzoic acid conversion into the corresponding sulfoxide by CYP199A4 isoforms. **(b)** HPLC analysis of the amount of the 4-ethylsulfinylbenzoic acid product (RT = 5.8 min) generated by the CYP199A4 isoforms over 240 minutes.

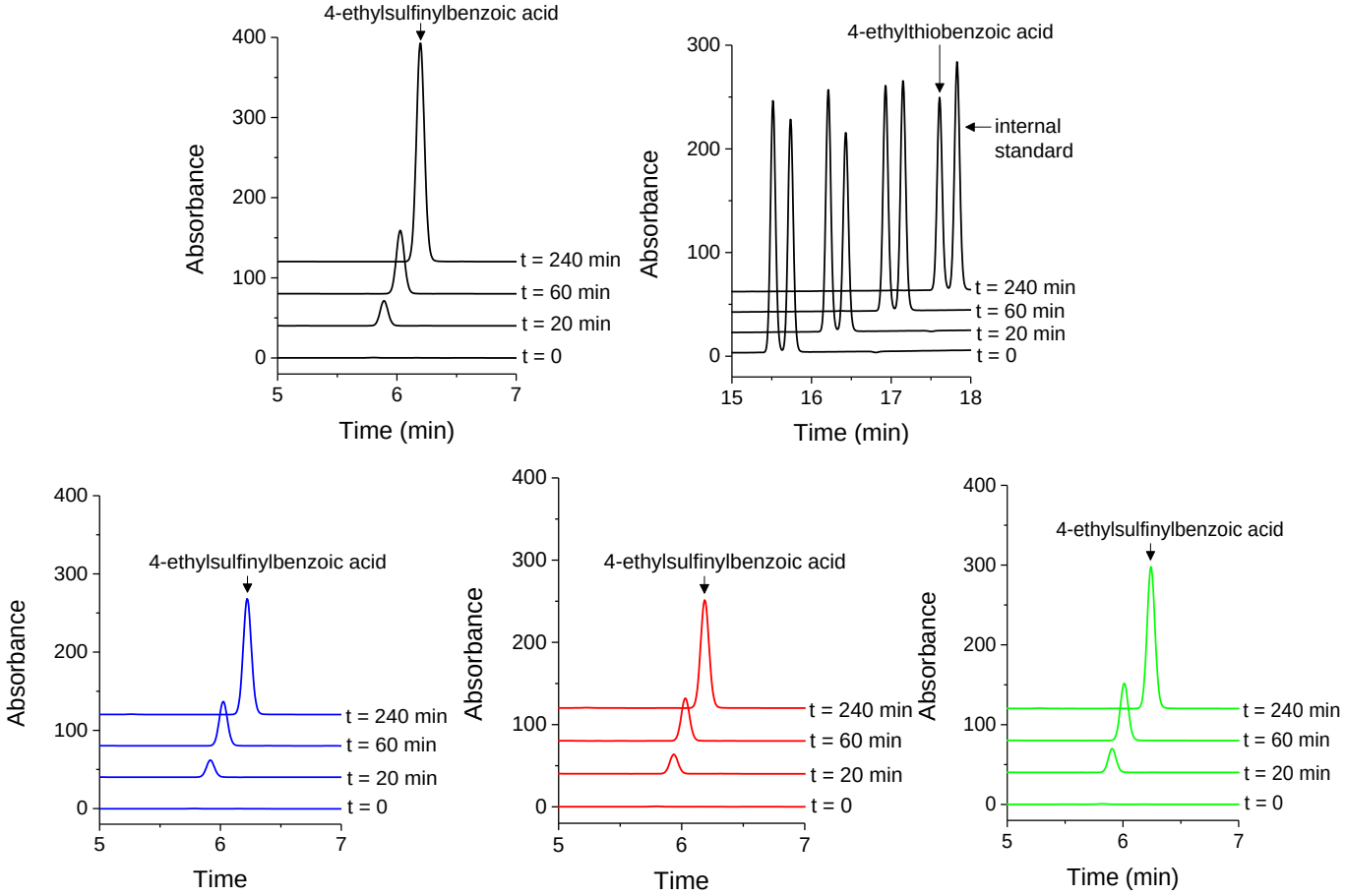

Figure S15. (b) Conversion of 4-ethylthiobenzoic acid into 4-ethylsulfinylbenzoic acid by WT CP199A4 (**blue**) and the T252E (**black**), D251N (**red**) and T252A (**green**) mutants over a 4-hour period. H_2O_2 (6 mM) was used as the oxygen donor. No 4-mercaptobenzoic acid was detected.

Table S5. Data collection, processing and refinement statistics for the crystal structures of the T252E mutant of CYP199A4 in complex with benzoic acid substrates.

	T252E$_{CYP199A4}$ + 4-methylthiobenzoic acid	**T252E$_{CYP199A4}$ + 4-ethylthiobenzoic acid**
PDB code	7TP6	7TP5
X-ray wavelength (Å)	0.95370	0.95370
Unit cell parameters (Å/°)	*a* = 41.1 *b* = 51.8 *c* = 80.0 α = 90.0 β = 92.3 γ = 90.0	*a* = 40.7 *b* = 51.5 *c* = 79.3 α = 90.0 β = 92.3 γ = 90.0
Space group	$P12_11$	$P12_11$
Molecules per asymmetric unit	1	1
Resolution range (Å)	43.46 – 1.66 (1.68 – 1.66)	40.70 – 1.66 (1.68 – 1.66)
<I/σ(I)>	7.4 (1.6)	9.3 (1.0)
Unique reflections	38747	31873
Completeness of data	96.3 (90.4)	81.1 (73.3)
Multiplicity	6.1 (5.1)	5.0 (4.3)
R_{merge} (all I+ and I−) (%)	16.7 (93.0)	14.5 (152.1)
R_{pim} (all I+ and I−) (%)	7.1 (44.0)	6.7 (76.3)
$CC_{1/2}$	99.1 (61.8)	99.4 (37.6)
R_{work} (%)	19.13	16.62
R_{free} (5% held) (%)	22.88	20.19
Ramachandran plot (%)		
Most favored	98.21	97.95
Allowed	1.79	2.05
Outliers	0	0
Unusual rotamers (%)	0.31	0.31
RMSD bond angles (°)	0.828	0.736
RMSD bond lengths (Å)	0.006	0.004
Omit map type, contour level, carve radius	composite omit map, 1.5 σ, 1.5 Å carve	feature-enhanced map, 1.0 σ, 1.5 Å carve

Values in parentheses correspond to the highest resolution (outer) shell.

Overlay of substrate-bound T252E and WT CYP199A4 structures

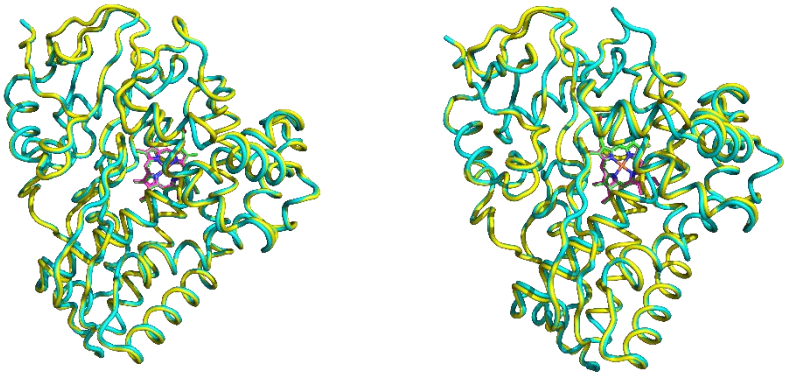

(a) 4-methylthiobenzoic acid (RMSD = 0.400 Å)

(b) 4-ethylthiobenzoic acid (RMSD = 0.396 Å)

Figure S16. Overlaid structures (Cα traces) of the T252E mutant (yellow cartoon, magenta heme) and WT CYP199A4 (blue cartoon, green heme) with various ligands bound. The RMSD between the Cα atoms is given below each figure (over all 393 pairs). The PDB codes are: 7TP6, 5KT1, 7TP5, and 5U6U.

T252E$_{CYP199A4}$ chloride binding sites

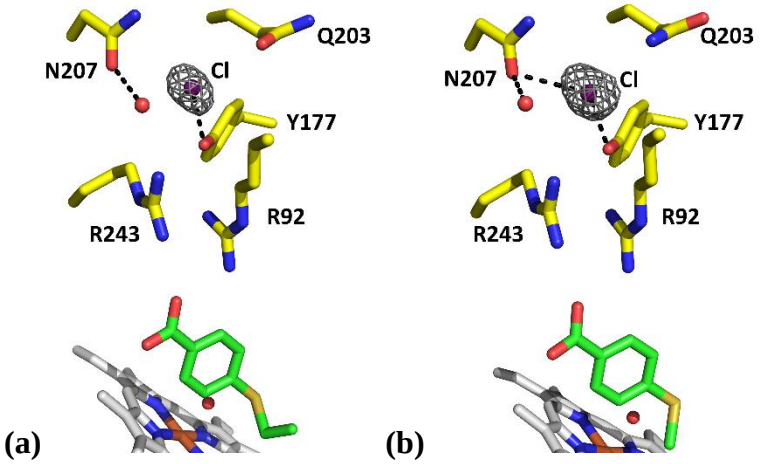

Figure S17. Chloride binding site of the T252E mutant of CYP199A4 in complex with **(a)** 4-ethylthioBA and **(b)** 4-methylthioBA. A *2mFo-DFc* composite omit map of the chloride ion (purple sphere) is shown as gray mesh contoured at 1.0 σ (1.5 Å carve). The PDB codes are 7TP5 and 7TP6.

Table S6. Distances and angles between notable features of the 4-methylthio- and 4-ethylthio-benzoate-bound T252E crystal structures. Values are also given for the WT structures for comparison (PDB: 5KT1 and PDB: 5U6U, respectively).[27] The ferryl oxygen of Cpd I was modelled 1.62 Å above the iron (along the axis defined by the Fe-S bond).

Distance	**4-methylthioBA-bound $T252E_{CYP199A4}$ (7TP6)**	**4-methylthioBA-bound $WT_{CYP199A4}$ (5KT1)**	**4-ethylthioBA-bound $T252E_{CYP199A4}$ (7TP5)**	**4-ethylthioBA-bound $WT_{CYP199A4}$ (5U6U)**
Fe - OH_2/OH^- ligand	2.2	Not present	2.1	Not present
Fe - C358 Sγ	2.3	2.5	2.3	2.4
Fe - C_{01}	4.8	4.5	5.4	5.2
Fe - C_{02}	-	-	6.9	6.7
Fe - S	5.1	5.0	4.9	4.8
Fe - closest O of E252	4.4	-	4.3	-
OH_2/OH^- ligand – closest O of E252	2.7	-	2.7	-
OH_2/OH^- ligand - C_{01}	3.6	-	4.2	-
OH_2/OH^- ligand - S	3.3	-	3.1	-
C_{01} - **O**=Fe	3.6	3.3	4.3	4.1
S - **O**=Fe	3.6	3.4	3.4	3.3
Angles (˚)				
Fe=**O**-C_{01}	125.4	131.9	126.3	127.0
Fe=**O**-S	154.0	162.5	150.0	152.0
Dihedral (C_{01}-S-C_{03}-C_{04})	-31.8	-33.9	-59.4	-55.2
C_{01}-S-C_{03}	101.7	104.3	105.2	106.1
Refined occupancies				
4-MethylthioBA/4-EthylthioBA substrate	96%		100%	
OH_2/OH^- ligand	80%	Not present	100%	Not present

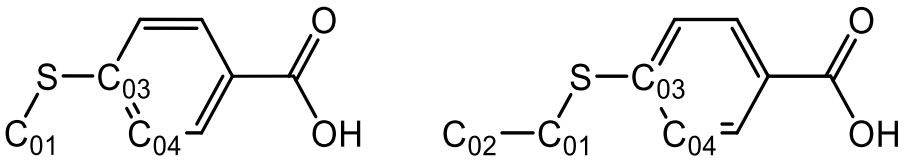

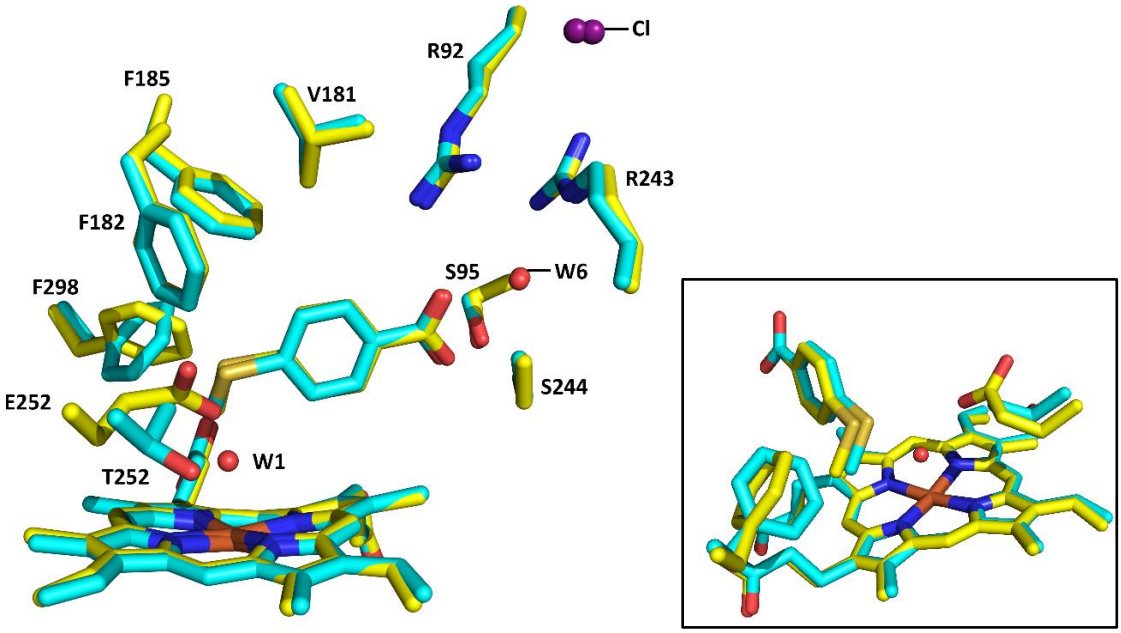

Figure S18a. Overlaid structures of WT (cyan; PDB ID: 5KT1) and T252E CYP199A4 (yellow; PDB code: 7TP6) with 4-methylthiobenzoate bound. The waters and chloride in the T252E structure are labeled.

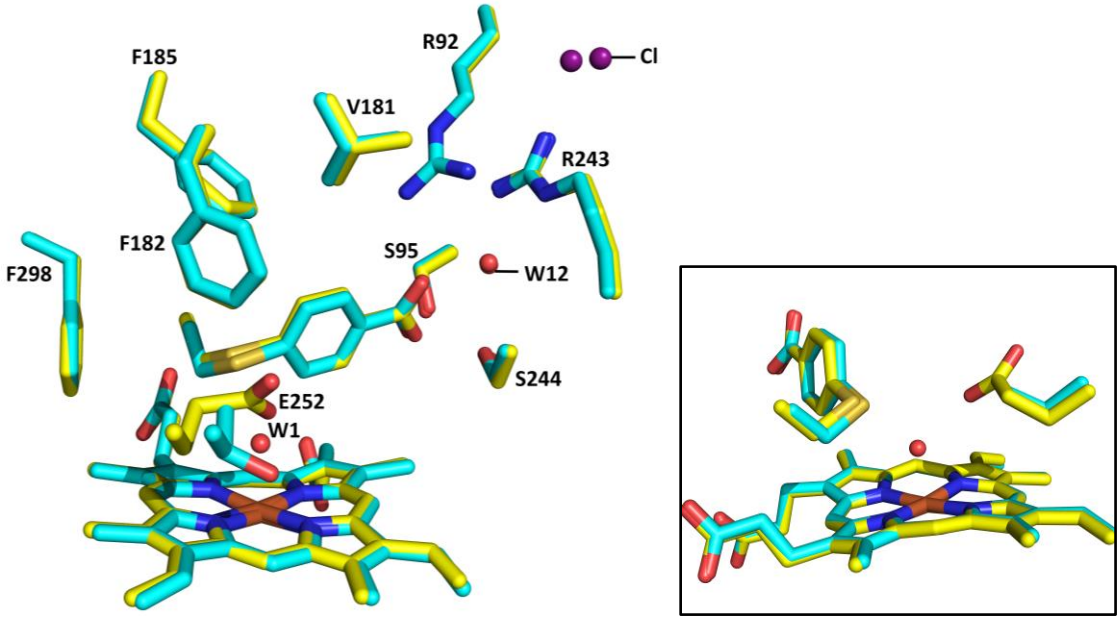

Figure S18b. Overlaid structures of WT (cyan; PDB ID: 5U6U) and T252E CYP199A4 (yellow; PDB code: 7TP5) with 4-ethylthiobenzoate bound. The waters and chloride in the T252E structure are labeled. The inset shows the binding orientation of 4-ethylthiobenzoic acid in the active site of each enzyme in more detail.

F298 conformation in the crystal structures of WT and T252E CYP199A4 bound to 4-methylthiobenzoic acid

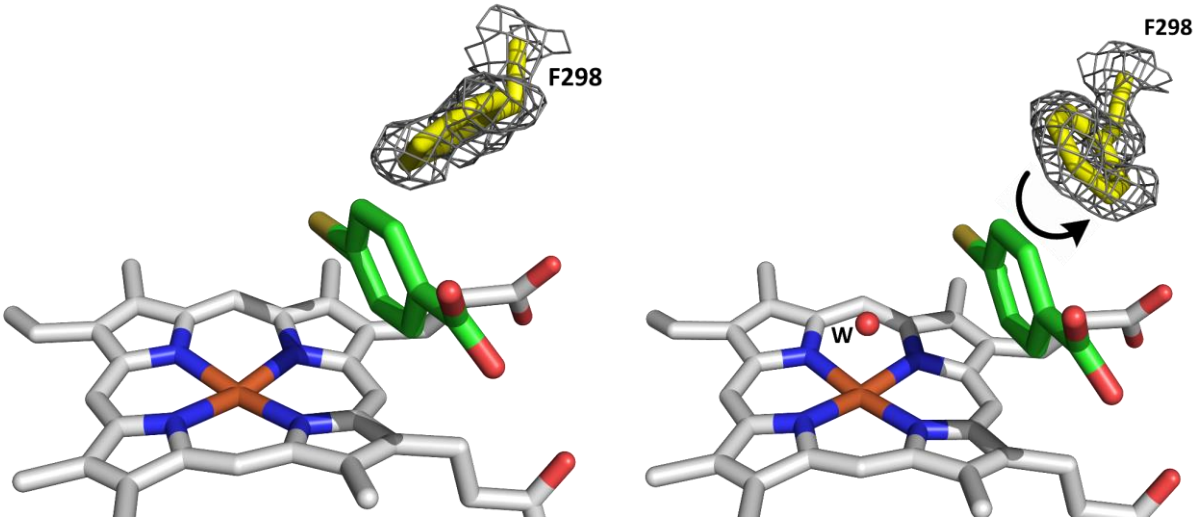

Figure S19a. Comparison of the F298 conformation in the crystal structures of WT and T252E CYP199A4 bound to 4-methylthiobenzoic acid. In the T252E structure, the F298 side chain is rotated (movement described by the black arrow). A *2mFo-DFc* feature-enhanced map of the F298 residue is shown as gray mesh contoured at 1.0 σ (1.5-Å carve).

The T252→E mutation altered the structure of the *I*-helix, including the position of the D251 and N255 residues.

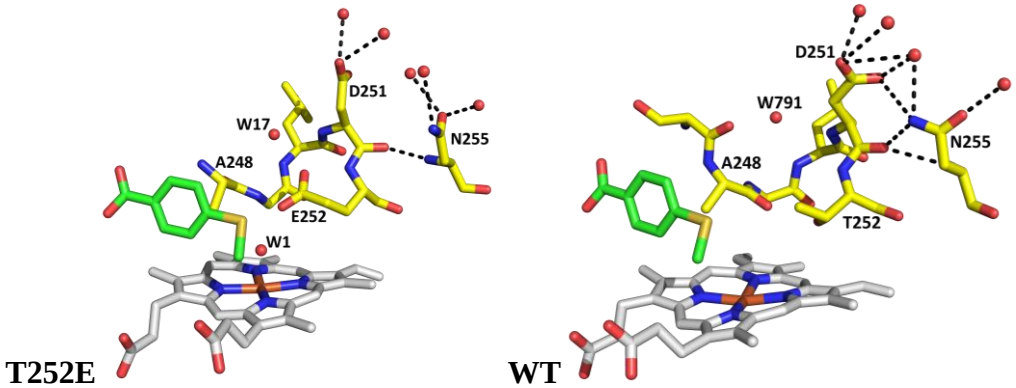

Figure S19b. Comparison of the oxygen-binding groove of T252E$_{CYP199A4}$ bound to 4-methylthiobenzoic acid (PDB code: 7TP6) and WT$_{CYP199A4}$ bound to 4-methylthiobenzoic acid (PDB code: 5KT1).

Table S7. Crystallographic data collection, processing and refinement statistic for the crystal structures of $D251N_{CYP199A4}$ and $T252A_{CYP199A4}$ in complex with 4-methylthiobenzoic acid. The space group is $P12_11$.

	$D251N_{CYP199A4}$ + 4-methylthiobenzoic acid	**$T252A_{CYP199A4}$ + 4-methylthiobenzoic acid**
PDB code	7TQM	8DYB
X-ray wavelength (Å)	0.95373	0.95370
Unit cell parameters (Å/°)	*a* = 44.54 *b* = 51.36 *c* = 79.05 α = 90.00 β = 92.32 γ = 90.00	*a* = 38.91 *b* = 50.94 *c* = 78.71 α = 90.00 β = 94.36 γ = 90.00
Space group	$P12_11$	$P12_11$
Molecules per asymmetric unit	1	1
Resolution range (Å)	44.50-1.44 (1.46 - 1.44)	42.73-1.88 (1.92 - 1.88)
<I/σ(I)>	8.0 (0.9)	11.4 (1.7)
Unique reflections	64061	25053 (1503)
Completeness of data	98.7 (90.0)	99.3 (93.7)
Multiplicity	6.9 (6.4)	7.5 (6.9)
R_{merge} (all I+ and I-) (%)	11.3 (169.8)	10.7 (93.1)
R_{pim} (all I+ and I-) (%)	4.6 (71.3)	4.2 (37.2)
$CC_{1/2}$	99.8 (64.0)	99.9 (72.4)
R_{work} (%)	18.06	22.57
R_{free} (5% held) (%)	20.48	26.21
Ramachandran plot (%)		
Most favored	97.95	96.68
Allowed	2.05	2.81
Outliers	0	0.51
Unusual rotamers (%)	0.91	1.25
RMSD bond angles (°)	0.797	0.713
RMSD bond lengths (Å)	0.006	0.004
Omit map type, contour level, carve radius	feature-enhanced map, 1.0 σ, 1.5 Å carve	feature-enhanced map, 1.0 σ, 1.5 Å carve

Values in parentheses correspond to the highest-resolution (outer) shell.

Overlay of substrate-bound T252A and WT CYP199A4 structures

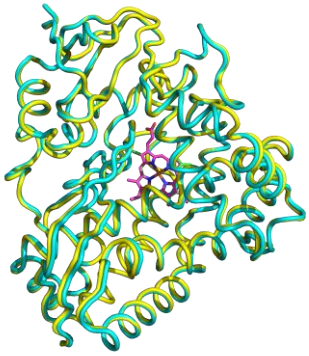

RMSD = 0.437 Å

Figure S20. Overlaid Cα traces of WT CYP199A4 (blue cartoon, green heme; PDB code: 5KT1) and the T252A mutant (yellow cartoon, magenta heme) bound to 4-methylthiobenzoic acid. The RMSD between Cα atoms is 0.437 Å (over all 393 pairs).

Overlay of substrate-bound D251N and WT CYP199A4 structures

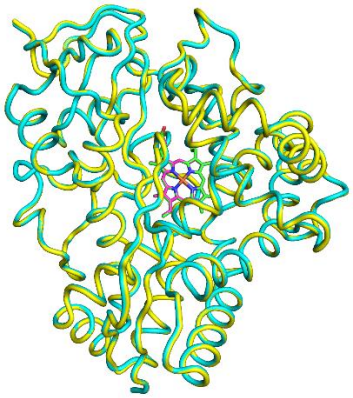

RMSD = 0.167 Å

Figure S21. Overlaid Cα traces of WT CYP199A4 (blue cartoon, green heme; PDB code: 5KT1) and the D251N mutant (yellow cartoon, magenta heme; PDB code: 7TQM) bound to 4-methylthiobenzoic acid. The RMSD between Cα atoms is 0.167 Å (over all 393 pairs).

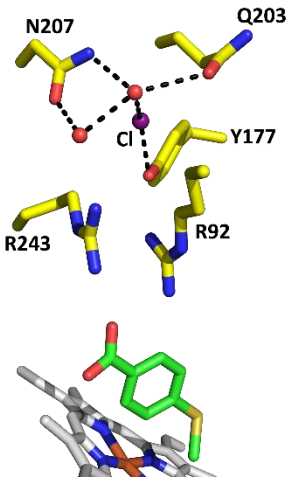

WT$_{CYP199A4}$ + 4-methylthiobenzoic acid (PDB code: 5KT1)

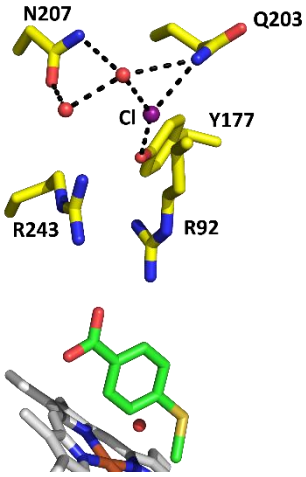

D251N$_{CYP199A4}$ + 4-methylthiobenzoic acid (PDB code: 7TQM)

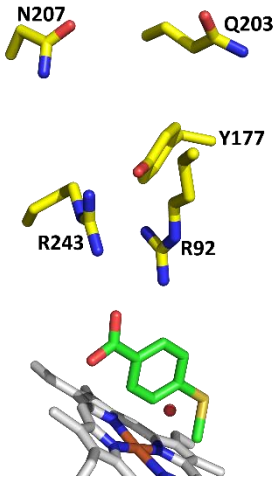

T252A$_{CYP199A4}$ + 4-methylthiobenzoic acid

Figure S22. The chloride binding site of WT$_{CYP199A4}$, D251N$_{CYP199A4}$ and T252A$_{CYP199A4}$ with 4-methylthiobenzoic acid bound. Note that no chloride ion has been modeled in the T252A crystal structure (there does not appear to be electron density at this position).

Table S8. Distances and angles in the crystal structures of 4-methylthiobenzoic acid-bound D251N$_{CYP199A4}$ and T252A$_{CYP199A4}$. Distances are also given for the equivalent WT$_{CYP199A4}$ structure for comparison (PDB code: 5KT1). The ferryl oxygen of Cpd I was modeled 1.62 Å above the iron (along the axis defined by the Fe-S bond). In the table, "W" refers to the heme-bound aqua ligand.

Distance (Å)	**4-methylthioBA-bound D251N$_{CYP199A4}$ (7TQM)**	**4-methylthioBA-bound T252A$_{CYP199A4}$**	**4-methylthioBA-bound WT$_{CYP199A4}$ (5KT1)**
Fe – W	2.3	2.5	Not present
Fe - C358 Sγ	2.3	2.6	2.5
W - S	3.3	3.3	Not present
W - C_{01}	3.6	3.3	Not present
Fe - C_{01}	4.6	4.2	4.5
Fe - S	5.1	5.1	5.0
C_{01} - **O**=Fe	3.5	3.1	3.3
S - **O**=Fe	3.6	3.6	3.4
Angles (°)			
Fe=**O**-C_{01}	122.3	123.4	131.9
Fe=**O**-S	151.7	153.2	162.5
Dihedral (C_{01}-S-C_{03}-C_{04})	-24.49	-20.96	-33.86
C_{01}-S-C_{03}	106.2	106.2	104.3
Refined occupancies (%)			
4-MethylthioBA	100%	100%	
Heme aqua ligand	W1 100%	W126 100%	Not present

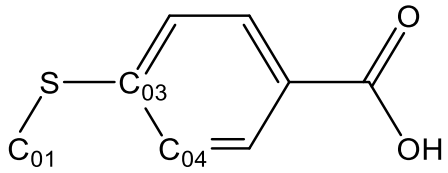

Measured S-Fe-OH_2 angle in the crystal structures of D251N, T252A and T252E CYP199A4 with 4-methylthiobenzoic acid bound

Table S9. Measured S_{Cys358}-Fe-OH_2 angle and Fe-O distances in the crystal structures of D251N, T252A and T252E CYP199A4 in complex with 4-methylthiobenzoic acid. The S-Fe-O angle in the D251N and T252E structures is closer to 180˚ (linear) than in the T252A structure. The overall coordinate error of each structure is also provided.

4-methylthiobenzoic acid			
CYP199A4 isoform	**S-Fe-O angle (˚)**	**Fe-O bond length (Å)**	**coordinate error**
D251N	168.6	2.31 ± 0.08	0.17
T252A	163.6	2.46 ± 0.27	0.26
T252E	172.8	2.17 ± 0.12	0.21
4-ethylthiobenzoic acid			
CYP199A4 isoform	**S-Fe-O angle (˚)**	**Fe-O bond length (Å)**	**coordinate error**
T252E	174.3	2.14 ± 0.14	0.17

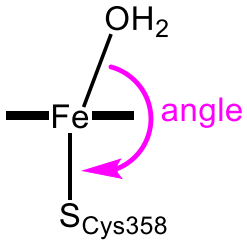

(a) T252A$_{CYP199A4}$ + 4-methylthiobenzoic acid

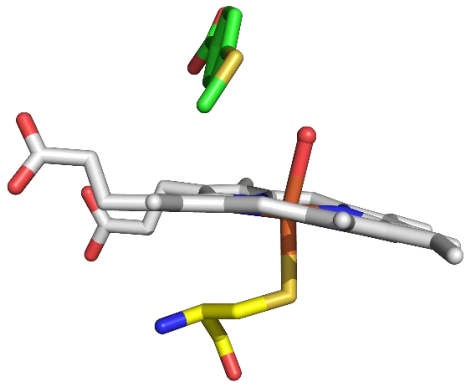

(b) T252E$_{CYP199A4}$ + 4-methylthiobenzoic acid

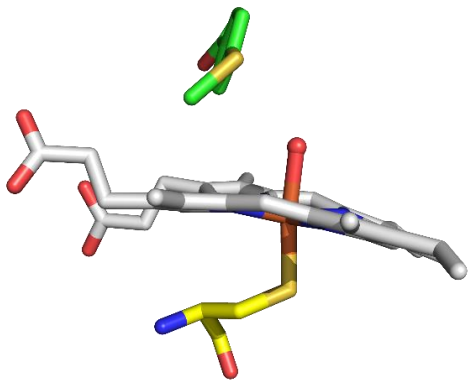

(c) D251N$_{CYP199A4}$ + 4-methylthiobenzoic acid

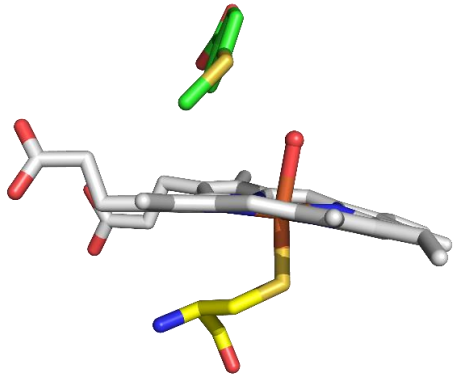

Figure S23. The S-Fe-O angle in the CYP199A4 mutant crystal structures with 4-methylthiobenzoic acid bound.

Comparison of the S-Fe-OH_2 angle in crystal structures of CYP199A4 isoforms bound to 4-methylthiobenzoic acid

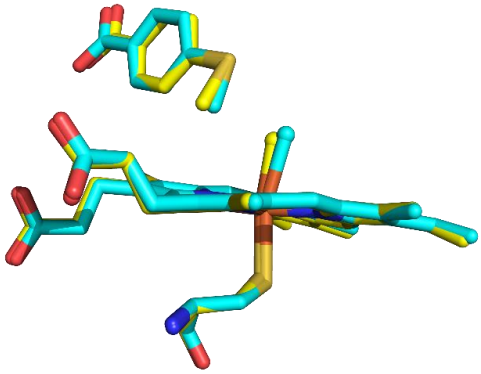

(a) Comparison of T252A (cyan) and D251N (yellow) structures

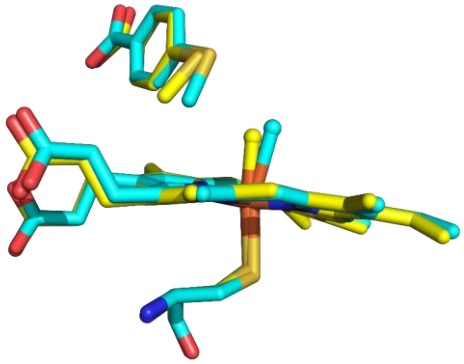

(b) Comparison of T252A (cyan) and T252E (yellow) structures

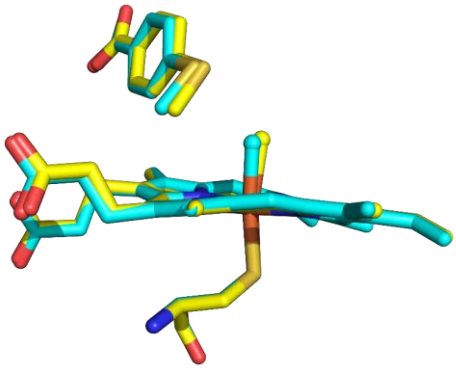

(c) Comparison of T252E (cyan) and D251N (yellow) structures

Figure S24. Comparison of the S-Fe-OH_2 angle in the crystal structures of T252A, D251N and T252E CYP199A4 bound to 4-methylthiobenzoic acid. The heme-bound water molecule is noticeably offset from the axis of the Fe-S bond in the T252A crystal structure. The Fe-O bond length is also longer in the T252A crystal structure (2.46 Å) than in the D251N (2.31 Å) or T252E (2.17 Å) structures.

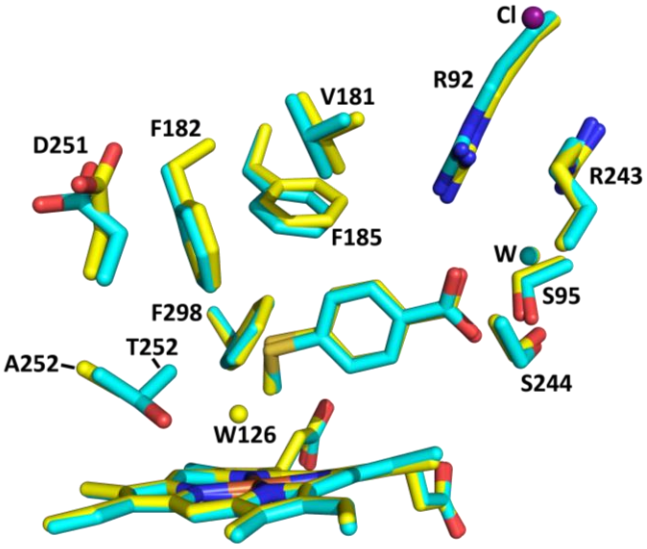

Figure S25. Overlaid structures of T252A$_{CYP199A4}$ (yellow) and WT$_{CYP199A4}$ (cyan; PDB code: 5KT1) in complex with 4-methylthiobenzoic acid. The chloride anion (purple sphere) in the WT structure is labeled. A heme-bound aqua ligand (W126) is only present in the T252A structure. The orientation of D251 differs in these two structures. (N255 also adopts a different conformation in the T252A structure). The position of the substrate in both structures is similar.

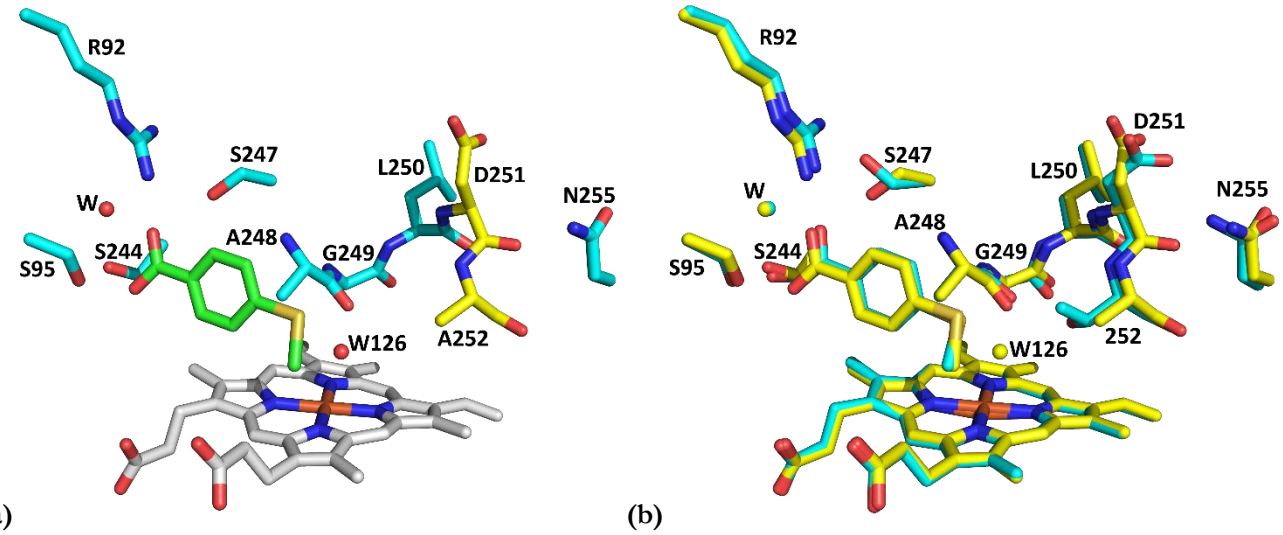

Figure S26. (a) The expanded active site of T252A$_{CYP199A4}$ bound to 4-methylthiobenzoic acid (green) including the oxygen binding groove. D251 and A252 are depicted in yellow. W126 is the heme-bound water ligand and is shown as a red sphere. **(b)** Overlaid crystal structures of T252A$_{CYP199A4}$ (yellow) and WT$_{CYP199A4}$ (cyan) bound to 4-methylthiobenzoic acid. Several active-site residues (e.g., D251, N255 and S247) have different orientations in the T252A structure. Waters are depicted as yellow or cyan spheres.

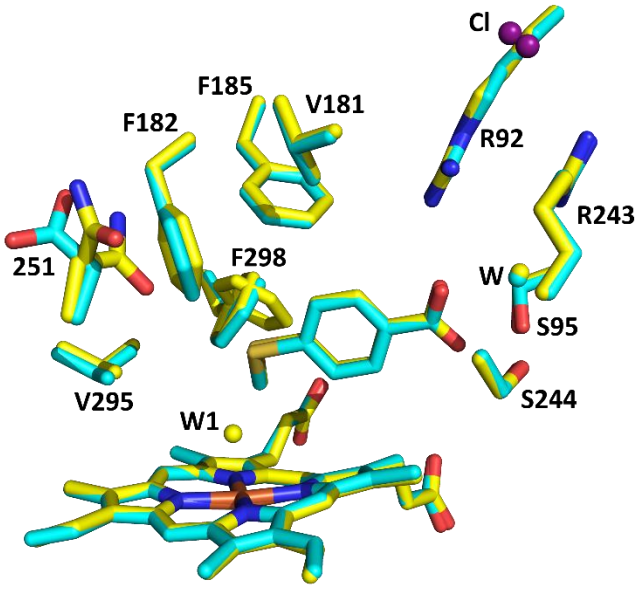

Figure S27. Overlaid crystal structures of 4-methylthiobenzoic acid-bound D251N$_{CYP199A4}$ (yellow; PDB code: 7TQM) and WT$_{CYP199A4}$ (cyan). In the WT structure (PDB code: 5KT1), the heme-bound water ligand has been expelled. The mutated residue (N251) and the side chain of F298 are shown in the two conformations in which they are present, see main text for details.

Overlaid crystal structures of D251N and T252E CYP199A4 bound to 4-methylthiobenzoic acid

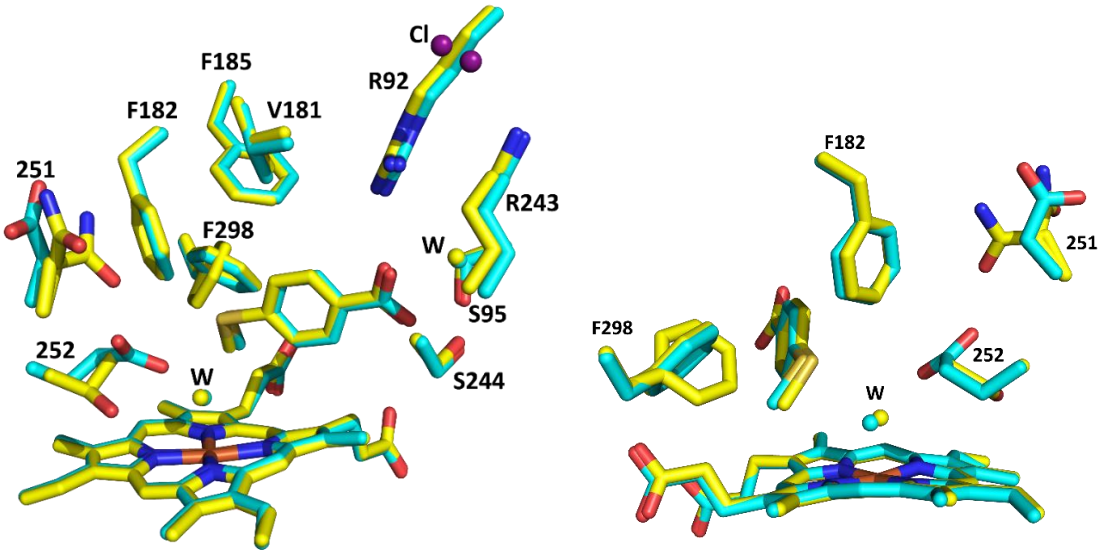

Figure S28. Overlaid crystal structures of 4-methylthiobenzoic acid-bound D251N$_{CYP199A4}$ (yellow; PDB code: 7TQM) and T252E$_{CYP199A4}$ (cyan; PDB code: 7TP6). In both structures there is a high-occupancy heme-bound aqua ligand (W) (100% and 80% occupancy). In the D251N structure, N251 and F298 are both present in two conformations.

N251 and F298 conformations in the crystal structure of D251N$_{CYP199A4}$ bound to 4-methylthiobenzoic acid

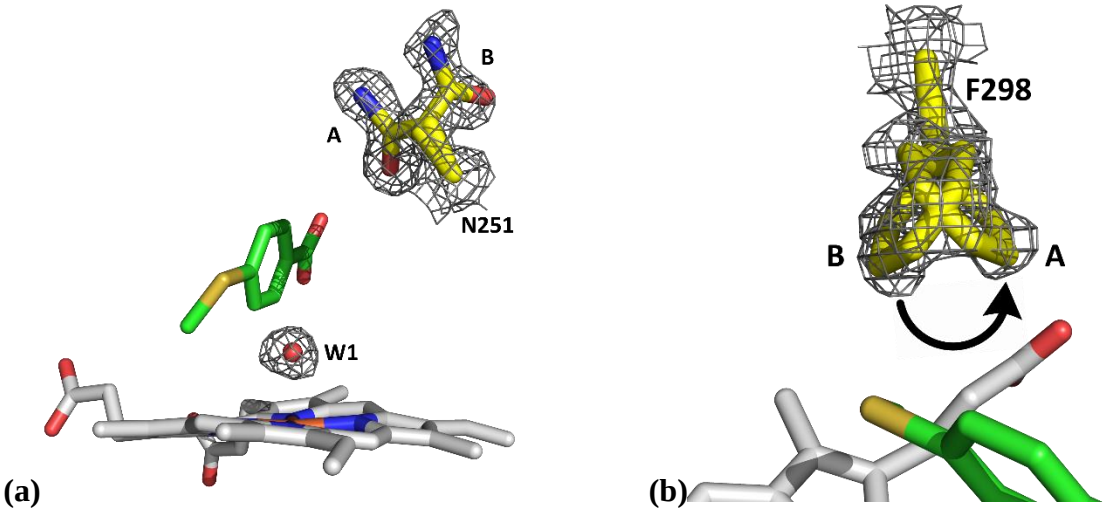

Figure S29. (a) In the 4-methylthiobenzoic acid-bound D251N$_{CYP199A4}$ crystal structure, N251 is present in two conformations. In one, the N251 side chain has rotated into the active site (conformation A; 60% occupancy). In the other, N251 points away from the active site, into the solvent channel (conformation B; 40% occupancy). A $2mF_o$-DF_c feature-enhanced map of N251 is shown as gray mesh contoured at 1.0 σ. **(b)** F298 is present in two conformations (46% (A) and 54% (B) occupancy) which are related by rotation of the phenyl ring (black arrow). A $2mF_o$-DF_c feature-enhanced map of F298 is shown as gray mesh contoured at 1.0 σ.

Heme conformation in the crystal structures of CYP199A4 isoforms in complex with 4-methoxybenzoic acid

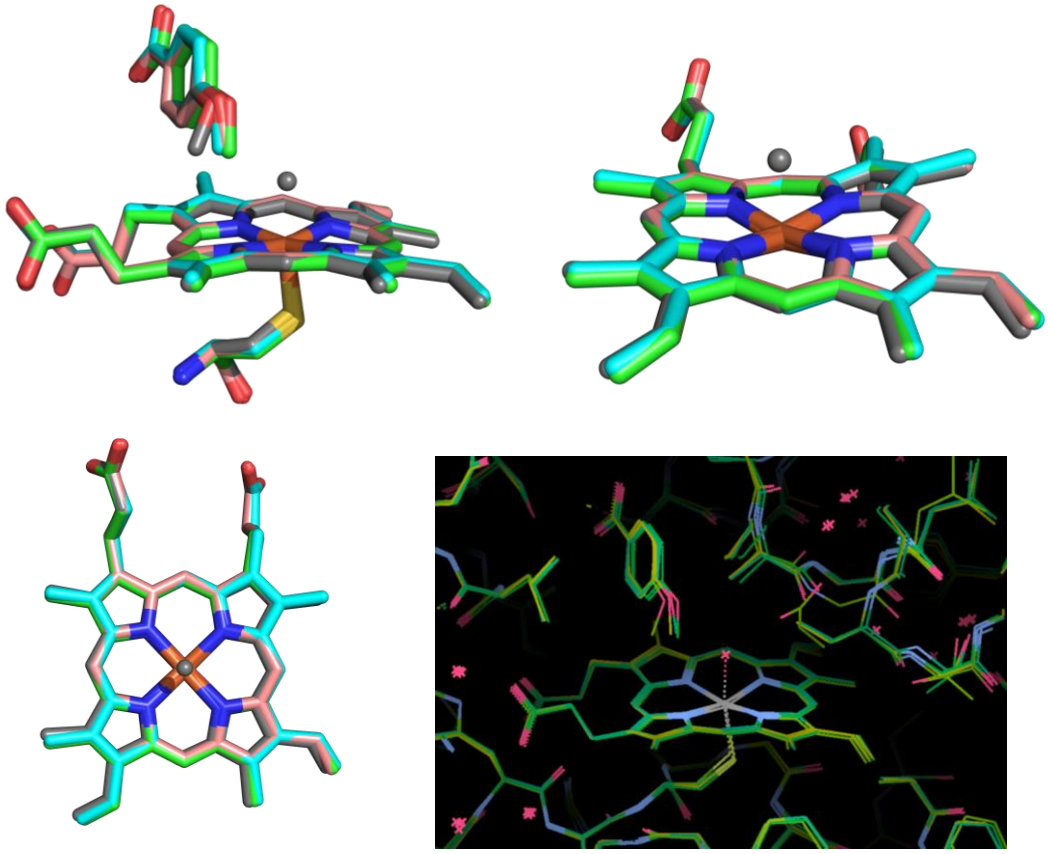

Figure S30. Overlaid heme groups in the crystal structures of WT (cyan; 4DO1), T252A (green; 5KDZ), D251N (salmon; 5KDY) and T252E (gray; 7REH) CYP199A4 bound to 4-methoxybenzoic acid.

Table S10 Measured heme iron position in the crystal structures of 4-methylthiobenzoic acid-bound WT, T252E, T252A and D251N CYP199A4

Crystal structure	Displacement of the iron out of the heme plane (plane defined by the four pyrrole nitrogens)	Displacement of the iron out of the heme plane (plane defined by all 24 atoms of the porphyrin)
WT + 4-methylthioBA (5KT1)	0.22	0.23
T252E + 4-methylthioBA (7TP6)	0.16	0.13
T252A + 4-methylthioBA (8DYB)	0.05	0.03
D251N + 4-methylthioBA (7TQM)	0.09	0.08

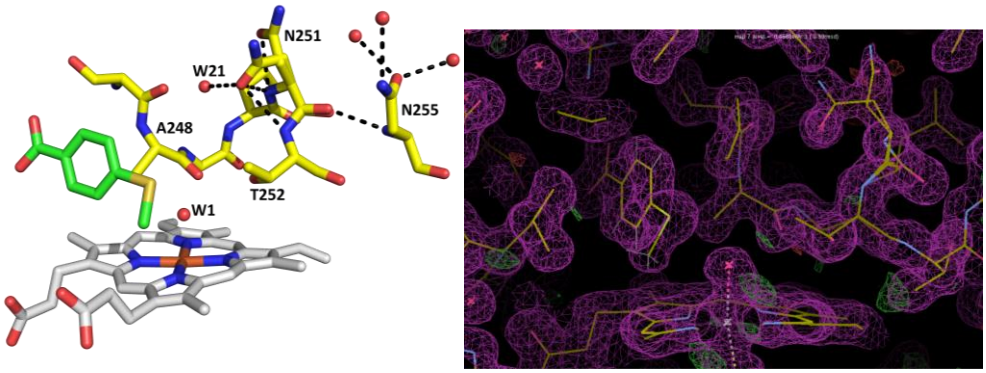

Figure S31 (a) D251N$_{CYP199A4}$ bound to 4-methylthiobenzoic acid (PDB code: 7TQM)

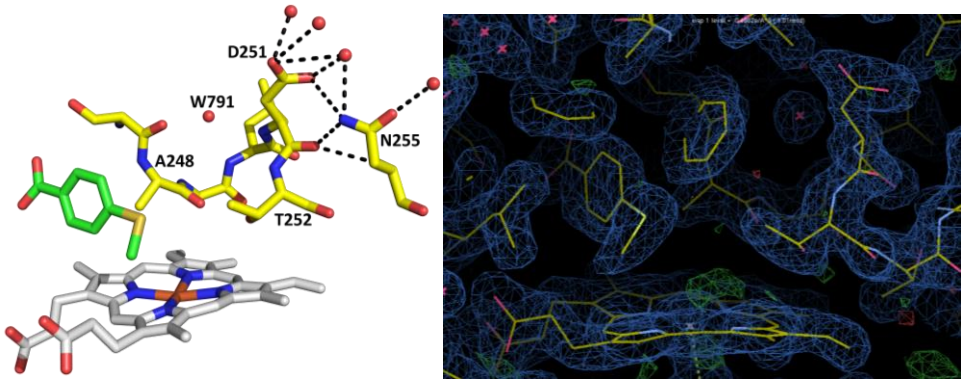

Figure S31 (b) WT$_{CYP199A4}$ bound to 4-methylthiobenzoic acid (PDB code: 5KT1)

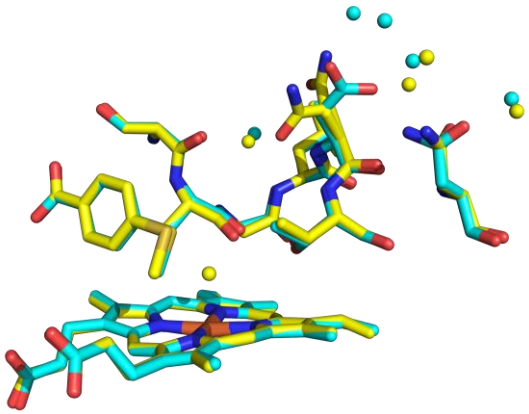

Figure S31 (c) Superimposed structures of 4-methylthiobenzoic acid-bound WT (cyan) and D251N (yellow) CYP199A4

In the D251N$_{CYP199A4}$ mutant, the mutated N251 side chain is present in two conformations. In one conformation, the N251 side chain has rotated into the active site (~60% occupancy). In this conformation, the asparagine side chain interacts with W21 (3.0 Å), the backbone NH of N251 (2.8 Å), and the backbone NH of T252 (3.0 Å). In the wild-type (WT) enzyme, the aspartate (D251) side chain interacts with N255 (3.5 Å). However, in the D251N mutant, the side chain of N255 has rotated by ~90˚ and does not interact with the N251 side chain.

The active-site structure of CYP199A4 is largely unaffected by the T252A, D251N and T252E mutations

Mutation of T252 to alanine or glutamate, or D251 to asparagine, did not appreciably alter the geometry of the active site of CYP199A4 nor the binding mode of 4-methoxybenzoic acid.

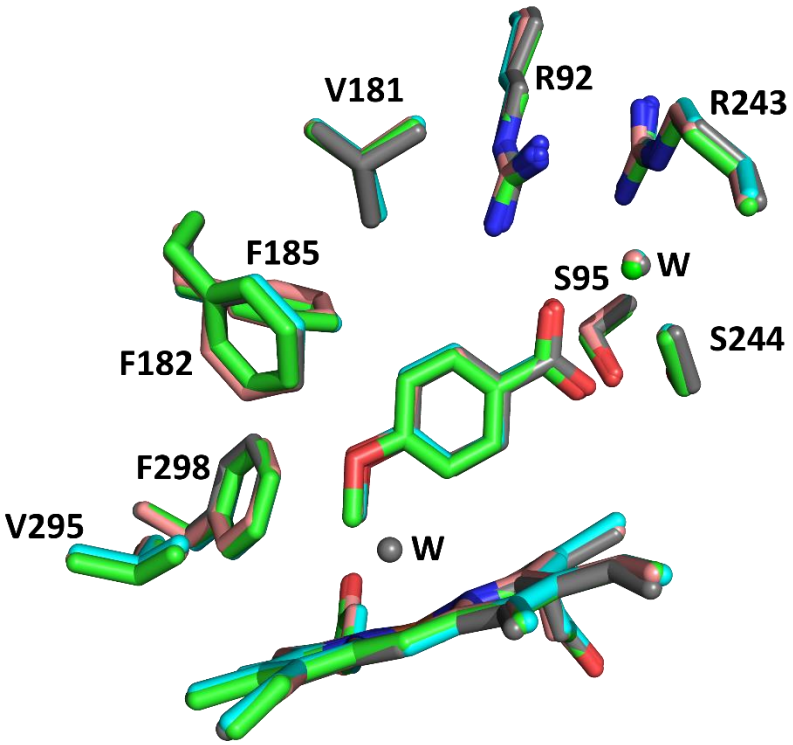

Figure S32. Active-site structure of WT CYP199A4 (cyan) and the T252E (gray), D251N (salmon) and T252A (green) isoforms in complex with 4-methoxybenzoic acid. These mutations do not appreciably alter the geometry of the active site nor the substrate binding mode. The D251N and T252A structures were reported previously (PDB codes: 5KDY and 5KDZ).

Comparison of the active-site structure of CYP199A4 isoforms bound to 4-methylthiobenzoic acid

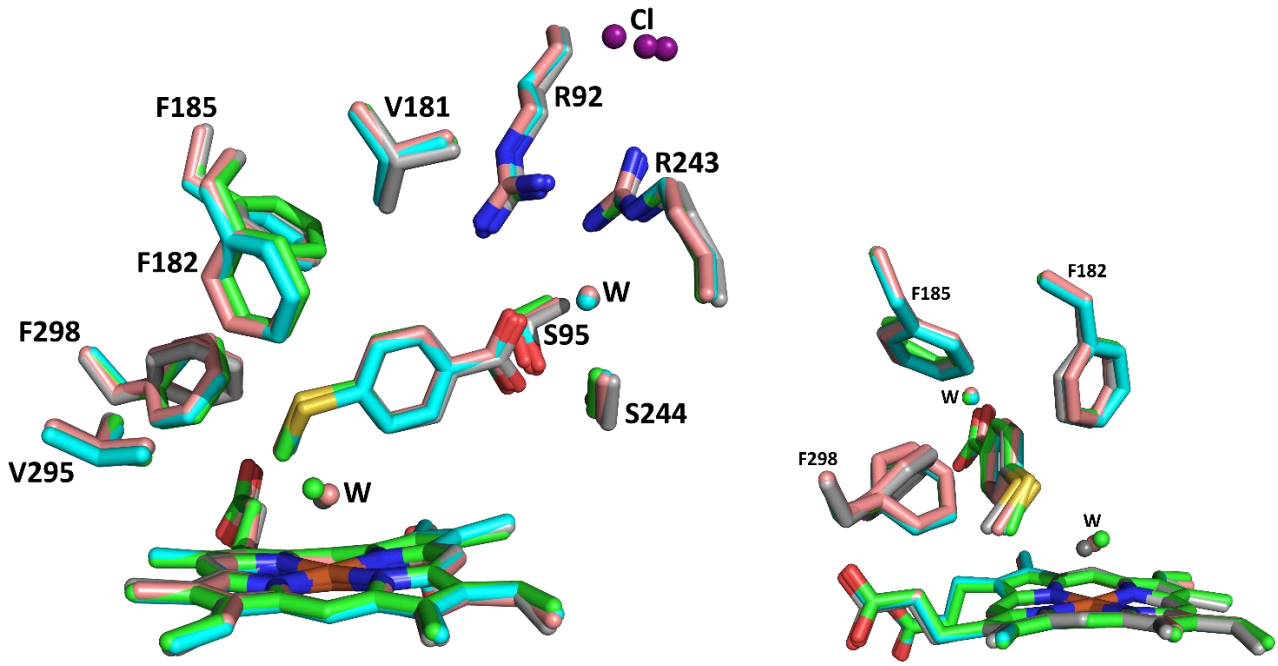

Figure S33. The active-site structure of WT CYP199A4 (cyan) and the T252E (gray), D251N (salmon) and T252A (green) mutants in complex with 4-methylthiobenzoic acid. The WT crystal structure was reported previously (PDB code: 5KT1).

A heme-bound aqua ligand is present in the T252E, D251N and T252A crystal structures. In contrast, in the WT crystal structure, the heme is pentacoordinate (the water ligand has been removed by the substrate).

Note that the side chain of F298 is found in different conformations in these structures.

In the T252A crystal structure, the heme-bound aqua ligand is noticeably offset from the axis of the Fe-S bond. The Fe-O bond length is also longer in the T252A structure compared to the T252E and D251N structures (2.46 Å *vs*. 2.17 Å and 2.31 Å).

Enantioselectivity of 4-ethylthiobenzoic acid sulfoxidation by CYP199A4 isoforms

Table S11. Enantioselectivity of NADH- and H_2O_2-supported sulfoxidation of 4-ethylthiobenzoic acid catalyzed by CYP199A4 isoforms.

	Substrate	Enantiomer 1	Enantiomer 2	1:2 ratio	% ee
Racemic sulfoxide	563.703	685.168	699.066	0.98	-
WT_NADH	431.497	390.919	36.872	10.60	83%
T252A_NADH	221.069	112.907	11.17	10.11	82%
T252E_NADH	790.379	35.652	6.839	5.21	68%
D251N_NADH	755.839	44.594	19.958	2.23	38%
WT_6 mM H_2O_2	621.171	56.754	32.382	1.75	27%
T252A_6 mM H_2O_2	3169.367	178.883	124.751	1.43	18%
T252E_6 mM H_2O_2	1850.834	79.859	55.354	1.44	18%
D251N_6 mM H_2O_2	2719.882	145.148	106.376	1.36	15%

Enantiomer numbering based on elution order.

Note that the true enantioselectivity of the H_2O_2-driven sulfoxidation reactions catalyzed by the CYP199A4 isoforms could not be determined. H_2O_2 alone can convert sulfides into sulfoxides. In the presence of H_2O_2, formation of racemic sulfoxide through uncatalyzed background oxidation of the sulfide would have occurred alongside the P450 reaction (Figure S33). The estimated enantioselective excess (±5%) if these was taken into account were 35% (T252E), >90% (WT), 35% (T252A) and 35% ee (D251N).

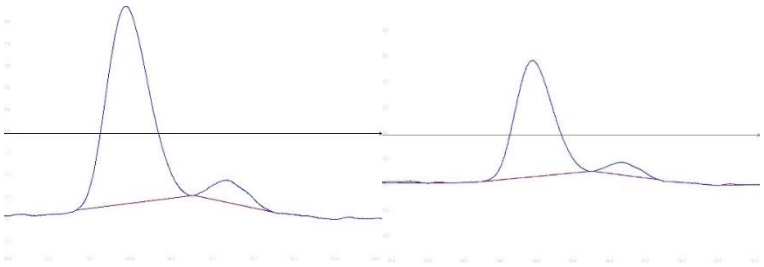

(a) WT_NADH (b) T252A_NADH

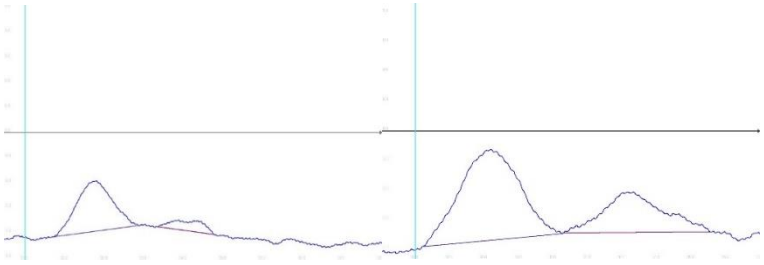

(c) T252E_NADH (d) D251N_NADH

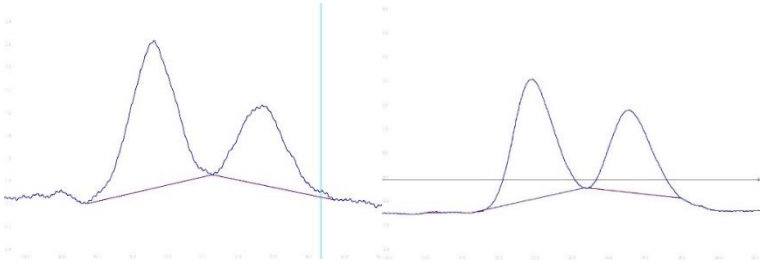

(a) WT_H_2O_2 (b) T252A_H_2O_2

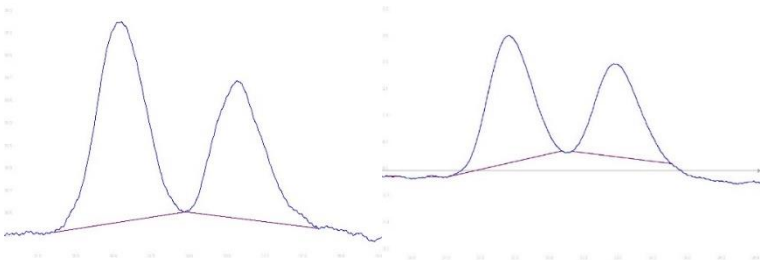

(c) T252E_H_2O_2 (d) D251N_H_2O_2

Figure S34. Chiral HPLC analysis of NADH- and H_2O_2-driven sulfoxidation of 4-ethylthiobenzoic acid catalyzed by CYP199A4 isoforms. In all cases, the major enantiomer was the first to elute.
Note that the measured enantioselectivity of the reactions is low for the H_2O_2-driven reactions. In the presence of H_2O_2, uncatalyzed conversion of 4-ethylthiobenzoic acid into racemic sulfoxide would have occurred alongside the P450 reaction. Because of this background oxidation, we could not accurately determine the true enantioselectivity of the CYP199A4-catalyzed reactions.

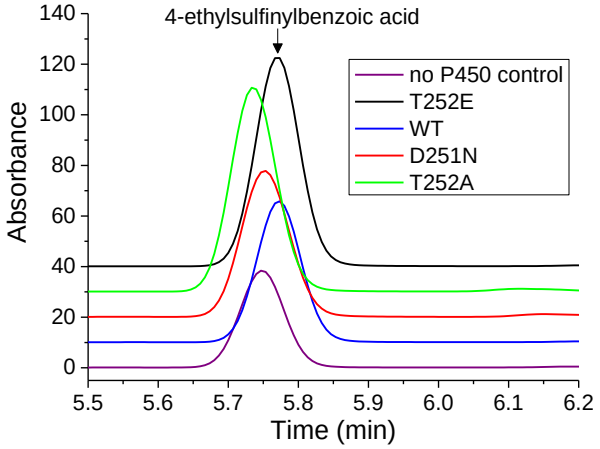

Figure S35. The amount of sulfoxidation of 4-ethylthiobenzoic acid that occurred over a 2-hour period in the presence of 6 mM H_2O_2 at room temperature, with or without P450 present. A substantial amount of sulfoxidation occurred when no P450 was present due to uncatalyzed oxidation by H_2O_2 (**purple**). A considerable portion of the sulfoxide in the T252E (**black**), WT (**blue**), D251N (**red**) and T252A (**green**) reactions would therefore be racemic sulfoxide resulting from background oxidation of the sulfide by H_2O_2.